BERKELEY LAB
LAWRENCE BERKELEY NATIONAL LABORATORY

Modeling Subsurface Scenarios: How Do We Do This?

Technical Workshop Series:
Technical Follow-up Discussion on Subsurface Modeling

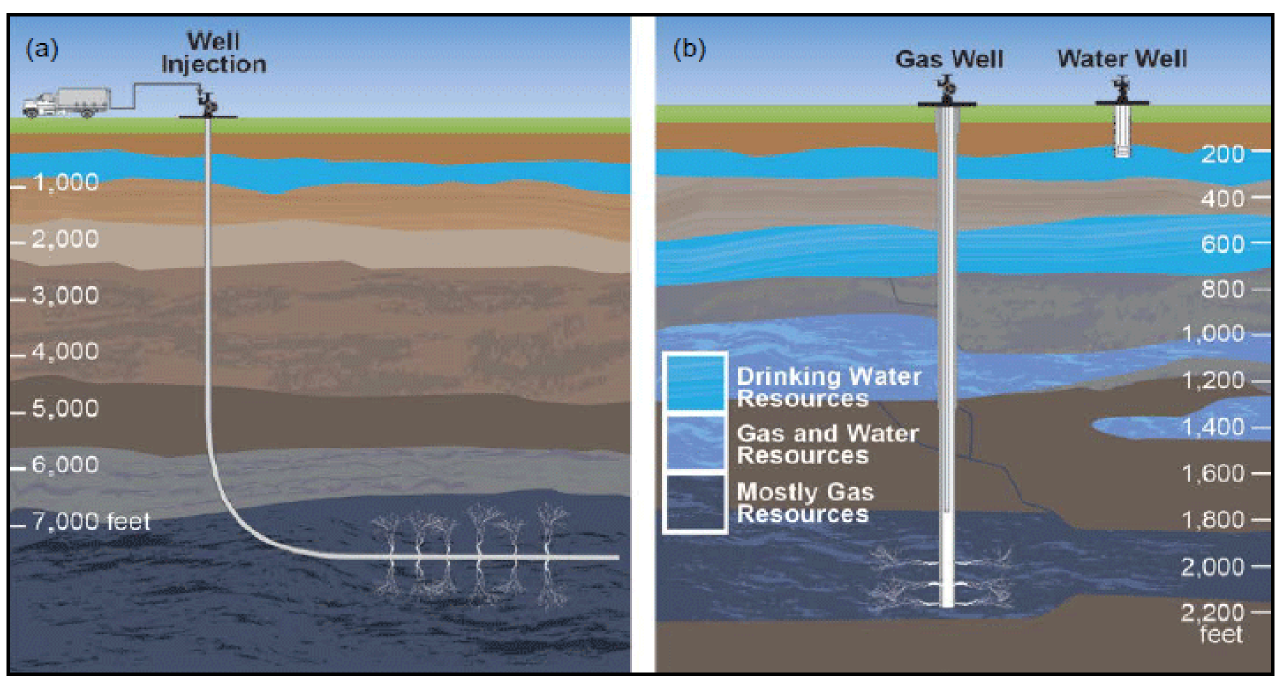

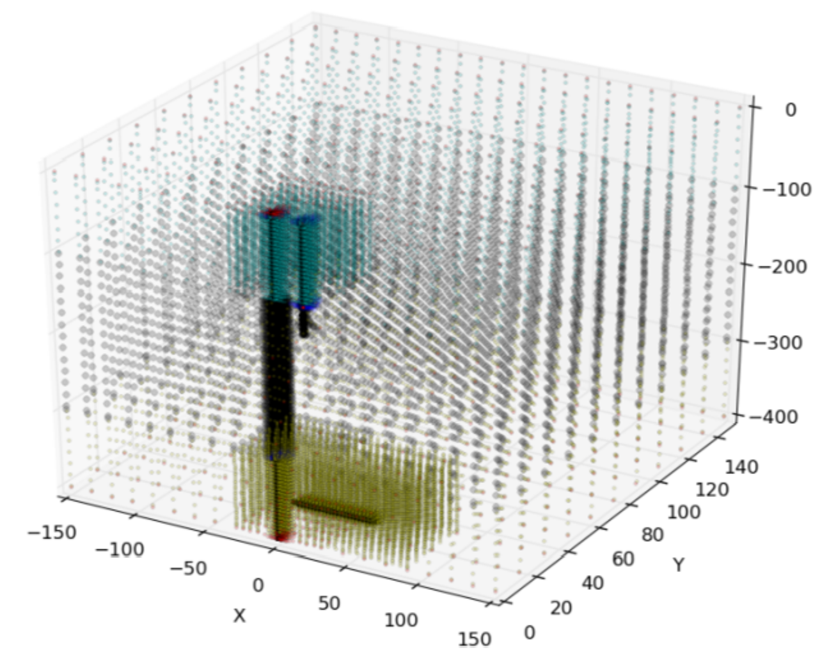

George J. Moridis, C. Matthew Freeman,
Jihoon Kim and Jonny Rutqvist

June 3, 2013

OUTLINE

Overall Approach

- Geomechanical question
- Flow and contaminant transport question

Modeling of Fluid Flow and Contaminant Transport

- The **TOUGH+RealGasH2O** code
- The **TOUGH+RealGasH2OCont** code

Modeling of Coupled Flow-Thermal-Geomechanical Processes

- Coupling with the **FLAC3D** code
- Coupling with the **ROCMECH** code

OVERALL APPROACH

- **Are the geomechanical failure (and fracture propagation) scenarios physically possible?**

- **If a fast transport pathway between the shale and the groundwater aquifer does exist, what is contaminant trans port affected by and what are the corrresponding time frames?**

OUTLINE

- **Background**
- **Code Description**
  - Fundamental equations
  - Capabilities
- **Validation Examples**
- **Applications Examples**

SIMULATION CODES

TOUGH+ Core Code with Options

- **Member of the TOUGH family of codes:**
  - Used by 400+ organizations in 65+ countries
  - Qualified code, Yucca Mountain project: flow, contaminant transport
- **FORTRAN 95/2003**
- **Object-Oriented Programming Structure**
- **Modular structure, ease of ex pansion, maximum traceability, UNICODE**

TOUGH+RealGasH2O (in review, C&G)

- **3D, non-isothermal**
- **Compositional (3 to 13 components): real gas mixture + H2O**
- **Darcy and non-Darcy flow, Knudsen diffusion, binary diffusion, sorption**
- **Fractured/unfractured media**

TOUGH+RGasH2OCont (in preparation)

- **3D, non-isothermal**
- **Compositional, 4 to 17 components: real gas mixture, oil, H2O, salt + solutes**
- **Halite precipitation**

NEEDED CAPABILITIES

- Darcy and non-Darcy flow through the matrix and fractures
- Inertial and turbulent effects (Klinkenberg effects)
- Real (as opposed to ideal) gas behavior
- Multi-phase flow (gas, aqueous, **organic phases** of fluids involved in hydraulic-fracturing); **variable viscosity (gels)**
- **Solute transport and density-driven flows (convection cells)**
- Mechanical dispersion, in addition to advection and molecular diffusion

Blue: RGasH2OCont

NEEDED CAPABILITIES (cont.)

- Gas sorption: three possible sorption models (linear, Langmuir or Freundlich), equilibrium or kinetic conditions
- **Sorption (primary and secondary) of contaminants (organic and solutes)** expected in fracturing processes: three possible sorption models (linear, Langmuir or Freundlich), equilibrium or kinetic conditions
- Coupled flow and thermal effects
- **Halite formation**: salt precipitation in brines caused by lower P and T; can significantly affect fracture and matrix permeability, and contaminant transport

Blue: RGasH2OCont

CODE DESCRIPTION

Fundamental Equations

$$\frac{d}{dt}\int_{V_n} M^{\kappa}\, dV = \int_{\Gamma_n} \mathbf{F}^{\kappa} \cdot \mathbf{n}\, dA + \int_{V_n} q^{\kappa}\, dV$$

Mass/heat balance

Mass accumulation

$$M^{\kappa} = \sum_{\beta \equiv A,G} \phi S_{\beta} \rho_{\beta} X^{\kappa}_{\beta} + \quad \delta_S (1-\phi)\rho_R \Psi^{i}, \quad \kappa = \mathrm{w}, g^{i} \; (i = 1, \ldots, N_G)$$

CODE DESCRIPTION

Fundamental Equations

Gas Sorption
Langmuir isotherm
Equilibrium and Kinetic

$$
\begin{cases}
\Psi^i = \dfrac{p_{dG} m_L}{p_{dG} + p_L} & \text{for ELaS} \\[2ex]
\dfrac{d\Psi^i}{dt} = k_L \left(\dfrac{p_{dG} m_L}{p_{dG} + p_L} - \Psi^i \right) & \text{for KLaS}
\end{cases}
$$

Multi-component

$$
\begin{cases}
\Psi^i = \dfrac{p_{dG} B^i m^i{}_L \Upsilon^i}{1 + p_{dG} \sum\limits_i B^i \Upsilon^i} & \text{for ELaS} \\[3ex]
\dfrac{d\Psi^i}{dt} = k_L^i \left(\dfrac{p_{dG} B^i m^i{}_L \Upsilon^i}{1 + p_{dG} \sum\limits_i B^i \Upsilon^i} - \Psi^i \right) & \text{for KLaS}
\end{cases}
$$

Additionally: Linear and Freundlich

Fundamental equations

Heat accumulation

$$M^{\theta} = (1-\varphi)\rho_R \int_{T_0}^{T} C_R(T)\, dT + \sum_{\beta=A,G} \varphi S_\beta \rho_\beta U_\beta + \delta_\Psi (1-\varphi)\rho_R \sum_{i=1}^{N_G} u^i Y^i$$

Flow terms

$$\mathbf{F}^{\kappa} = \sum_{\kappa \equiv A,G} \mathbf{F}^{\kappa}_{\beta} \qquad \kappa \equiv w, g^i \ (i \geq 1)$$

$$\mathbf{F}_\beta = \rho_\beta \left[-\frac{k\, k_{r\beta}}{\mu_\beta} \nabla \Phi_\beta \right] = \rho_\beta\, \mathbf{v}_\beta \,, \text{ where } \nabla \Phi_\beta = \nabla P_\beta - \rho_\beta\, \mathbf{g}$$

Fundamental equations

Gas Flow: Inertial, slippage, diffusion effects

$$\mathbf{F}_G^{\kappa} = \left(1 + \frac{b}{P_G}\right)\rho_G \mathbf{v}_G X_G^{\kappa} + \mathbf{J}_G^{\kappa}, \quad \kappa = \mathrm{w}, g_i \ (i \geq 1)$$

$$\mathbf{J}_G^{\kappa} = -\phi S_G \left(\phi^{1/3} S_G^{7/3}\right) D_G^{\kappa} \rho_G \nabla X_G^{\kappa} = -\phi S_G \left(\tau_G\right) D_G^{\kappa} \rho_G \nabla X_G^{\kappa}, \quad \kappa = \mathrm{w}, g^i \ (i \geq 1)$$

$$\frac{b}{P_G} = (1 + \alpha K_n)\left(1 + \frac{4K_n}{1 + K_n}\right) - 1$$

Knudsen diffusion

$$K_n = \frac{\bar{\lambda}}{r_{pore}} = \frac{\sqrt{\pi/2}\,\frac{1}{P_G}\,\mu_G \sqrt{\frac{RT}{M}}}{2.81708\sqrt{\frac{k}{\phi}}}$$

$$\alpha = \frac{128}{15\pi^2}\tan^{-1}\left[4\ K_n^{\ 0.4}\right]$$

Fundamental equations

Dusty gas model (multi-component diffusion)

$$\sum_{j=1,\, j\neq i}^{N_G} \frac{Y^i N_D^j - Y^j N_D^i}{D_e^{ij}} - \frac{N_D^i}{D_K^i} = \frac{p^i \nabla Y^i}{ZRT} + \left(1 + \frac{kp}{\mu_G D_K^i}\right)\frac{Y^i \nabla p^i}{ZRT}$$

Non-Darcy Flow Options: Forchheimer equation

$$\nabla\Phi_\beta = -\left(\frac{\mu_\beta}{k\, k_{r\beta}}\mathbf{v}_\beta + \beta_\beta\, \rho_\beta\, \mathbf{v}_\beta \left|\mathbf{v}_\beta\right|\right) \Rightarrow \mathbf{v}_\beta = \frac{2\nabla\Phi_\beta}{\frac{\mu_\beta}{k\, k_{r\beta}} + \sqrt{\left(\frac{\mu_\beta}{k\, k_{r\beta}}\right)^2 + 4\beta_\beta\, \rho_\beta \left|\nabla\Phi_\beta\right|}}$$

Additional Non-Darcy Option: Barree and Conway model (2007)

Fundamental equations

Heat Flow

$$\mathbf{F}^{\theta} = -\bar{k}_{\theta} \nabla T + f_{\sigma} \sigma_0 \nabla T^4 + \sum_{\beta \equiv A, G} h_{\beta} \mathbf{F}_{\beta}$$

Sources and Sinks

$$\hat{q}^{\kappa} = \sum_{\beta \equiv A,G} X_{\beta}^{\kappa} q_{\beta}, \quad \kappa = \mathrm{w}, g^{i} \ (i = 1, \ldots, N_G); \quad \hat{q}^{\theta} = \sum_{\beta \equiv A,G} q_{\beta} h_{\beta}$$

H2O Properties: Steam tables (IFC, 1967; NIST, 2000)

Real gas mixture properties: Cubic equations of state (RK, SRK, PR), 11 component library (Moridis et al., 2008; WebGasEOS)

TOUGH+ Modeling

- **Minimum of assumptions**
- **All known processes accounted for**

VALIDATION EXAMPLES

Problem V1: Real gas flow in a cylindrical reservoir

SPECIFICS

Data Type	Values
Matrix permeability k	3.04×10^{-14} m^2 (30.4 mD)
Reservoir thickness h	10 m
Well radius r_w	0.059 m
Reservoir radius r_e	100 m
Reservoir pressure p	10 MPa
Reservoir temperature T	60 ^{o}C
Reservoir porosity ϕ	0.30
Rock compressibility	2×10^{-10} 1/Pa
Gas composition	100% CH_4
Gas EOS	Peng-Robinson

Analytical solution of Fraim & Wattenbarger (1986) using pseudo-pressure concept

VALIDATION EXAMPLES

Problem V1: Real gas flow in a cylindrical reservoir

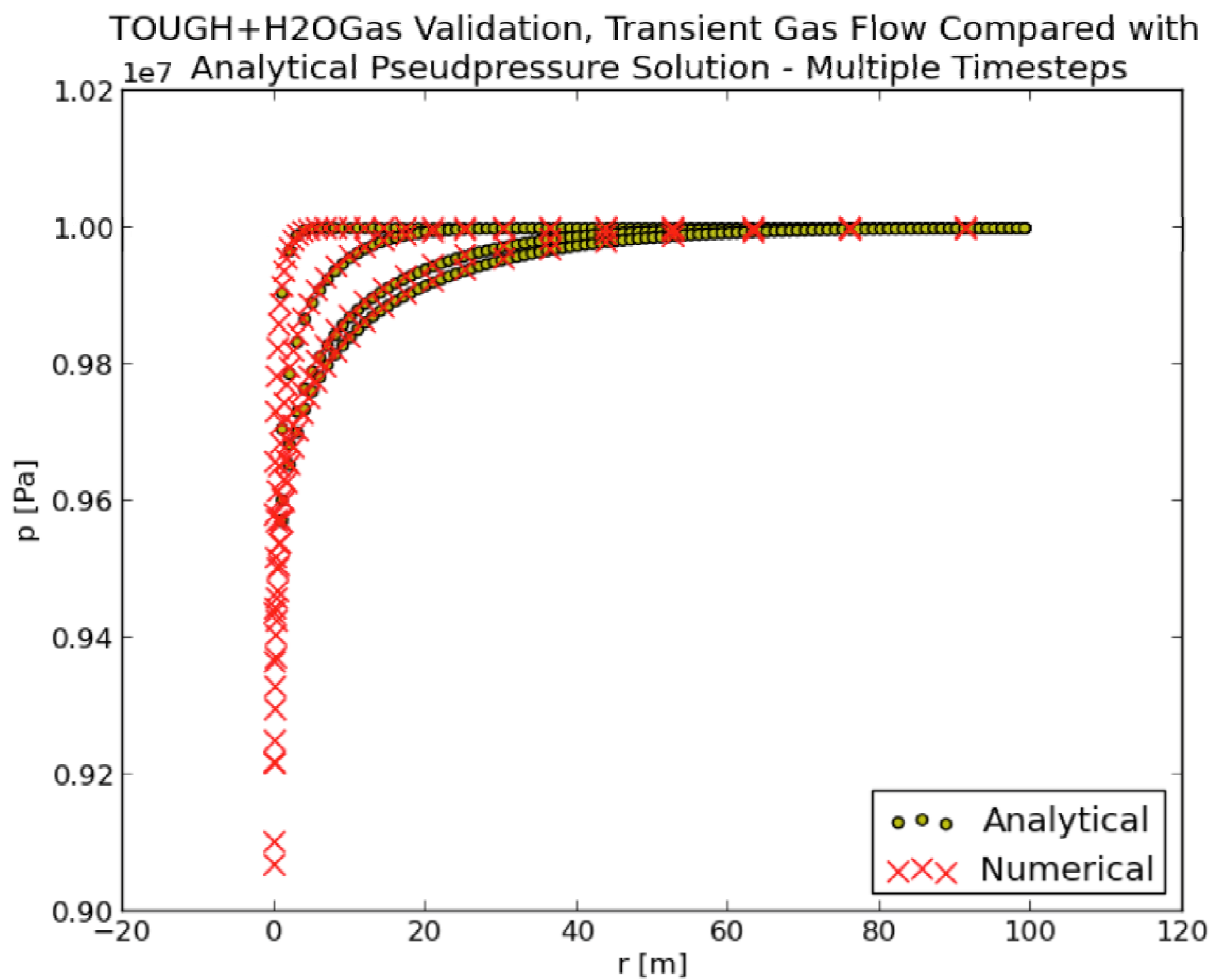

VALIDATION EXAMPLES

Problem V2: Water flow in a cylindrical reservoir

SPECIFICS

Data Type	Values
Matrix permeability k	3.04×10^{-14} m^2 (30.4 mD)
Reservoir thickness h	10 m
Well radius r_w	0.059 m
Reservoir radius r_e	100 m
Reservoir pressure p	10 MPa
Reservoir temperature T	30 °C
Reservoir porosity ϕ	0.30
Total compressibility c_t	4.88×10^{-10} 1/Pa
Gas EOS	Peng-Robinson

Analytical solution of Blasingame (1993) – pseudo-steady state

VALIDATION EXAMPLES

Problem V2: Water flow in a cylindrical reservoir

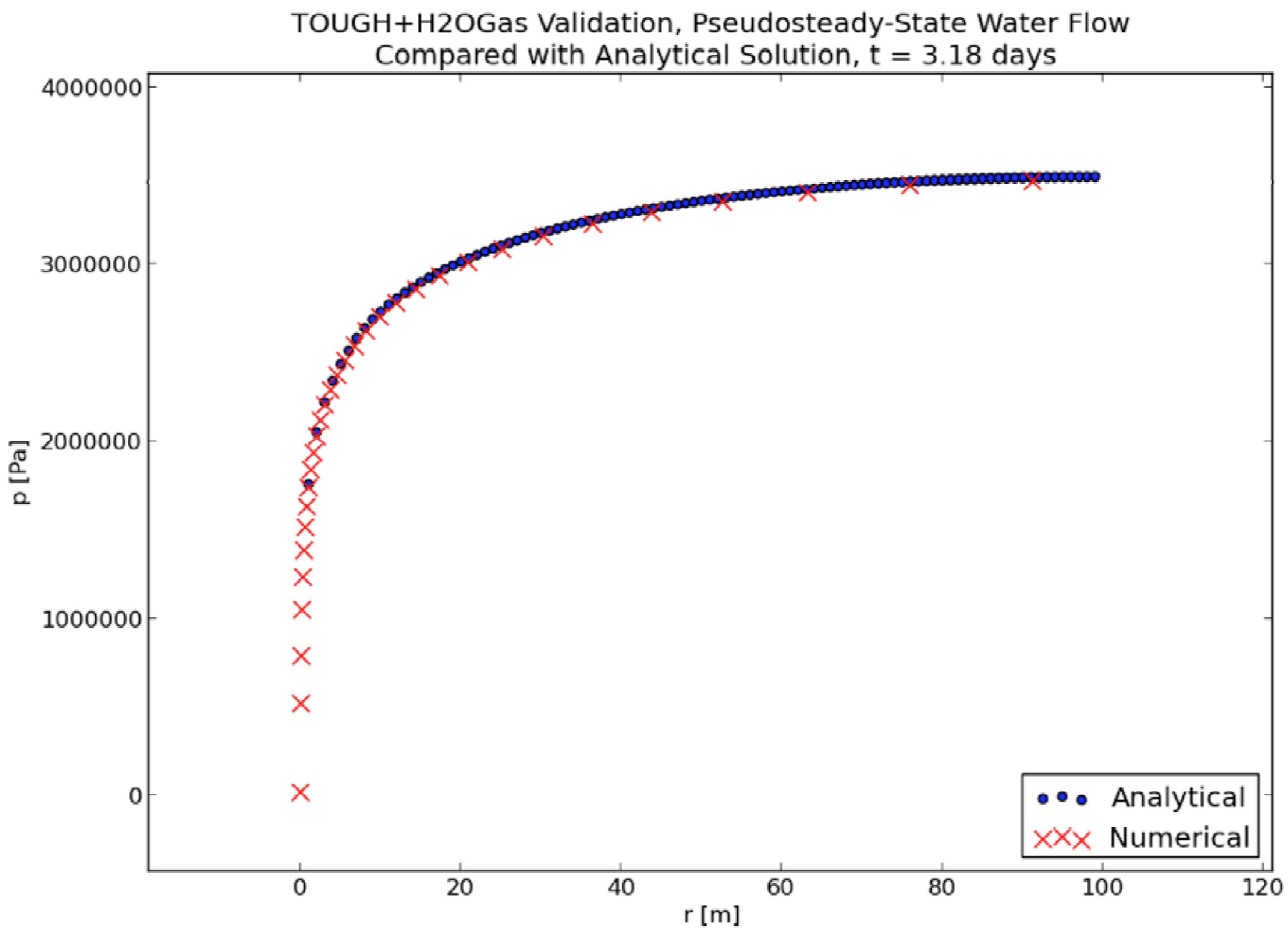

VALIDATION EXAMPLES

Problem V3: Gas flow in a tight gas reservoir with vertical well intersecting a vertical fracture plane

SPECIFICS

Data Type	Values
Matrix permeability k	3.08×10^{-19} m^2 (30.8 nD)
Fracture permeability k_f	6.68×10^{-14} m^2 (0.668 D)
Fracture half-length	20 m
Reservoir thickness h	10 m
Well radius r_w	0.05 m
Well pressure p_w	5 MPa
Reservoir pressure p	10 MPa
Reservoir temperature T	60 ^oC
Reservoir porosity ϕ	0.10
Rock compressibility	2×10^{-10} 1/Pa
Gas composition	100% CH_4
Gas EOS	Peng-Robinson

Analytical solutions of Cinco-Ley et al. (1978) and Cossio (2012)

VALIDATION EXAMPLES

Problem V3: Gas flow in a tight gas reservoir with vertical well intersecting a vertical fracture plane

Point cloud of pressure distribution

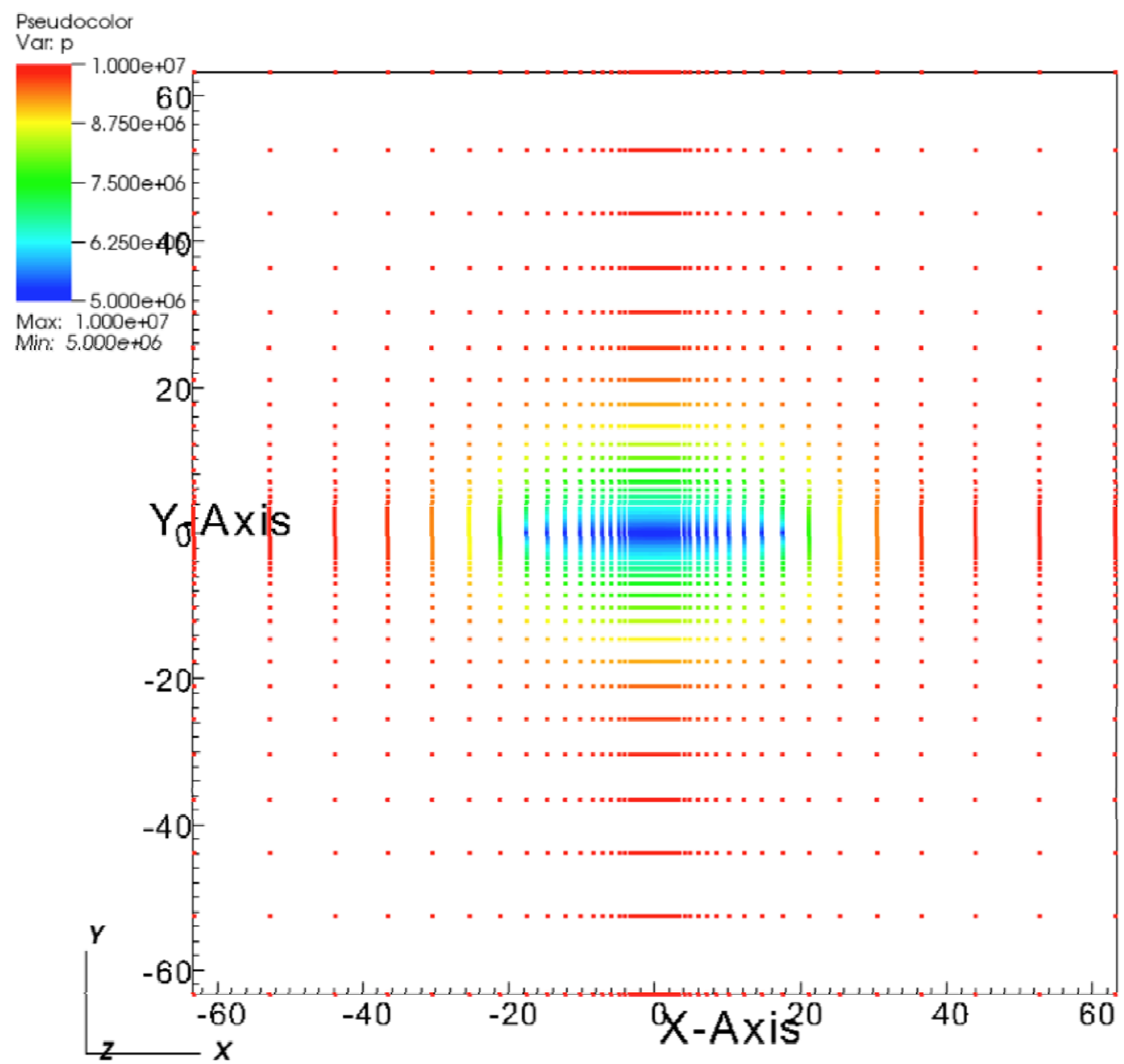

VALIDATION EXAMPLES

Problem V3: Gas flow in a tight gas reservoir with vertical well intersecting a vertical fracture plane

Contour plot of pressure distribution

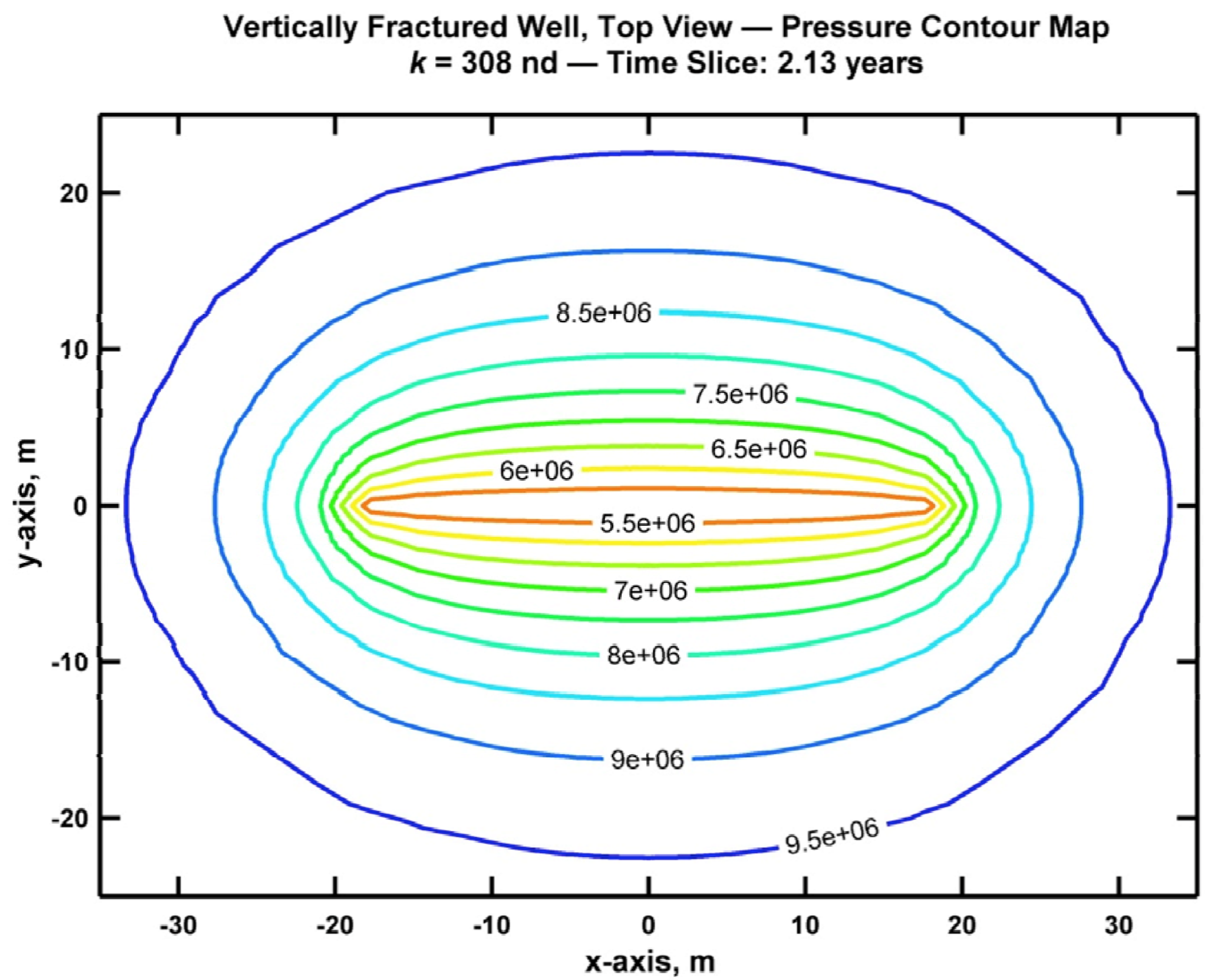

VALIDATION EXAMPLES

Problem V3: Gas flow in a tight gas reservoir with vertical well intersecting a vertical fracture plane

Production rate predictions: identical results (2 curves)

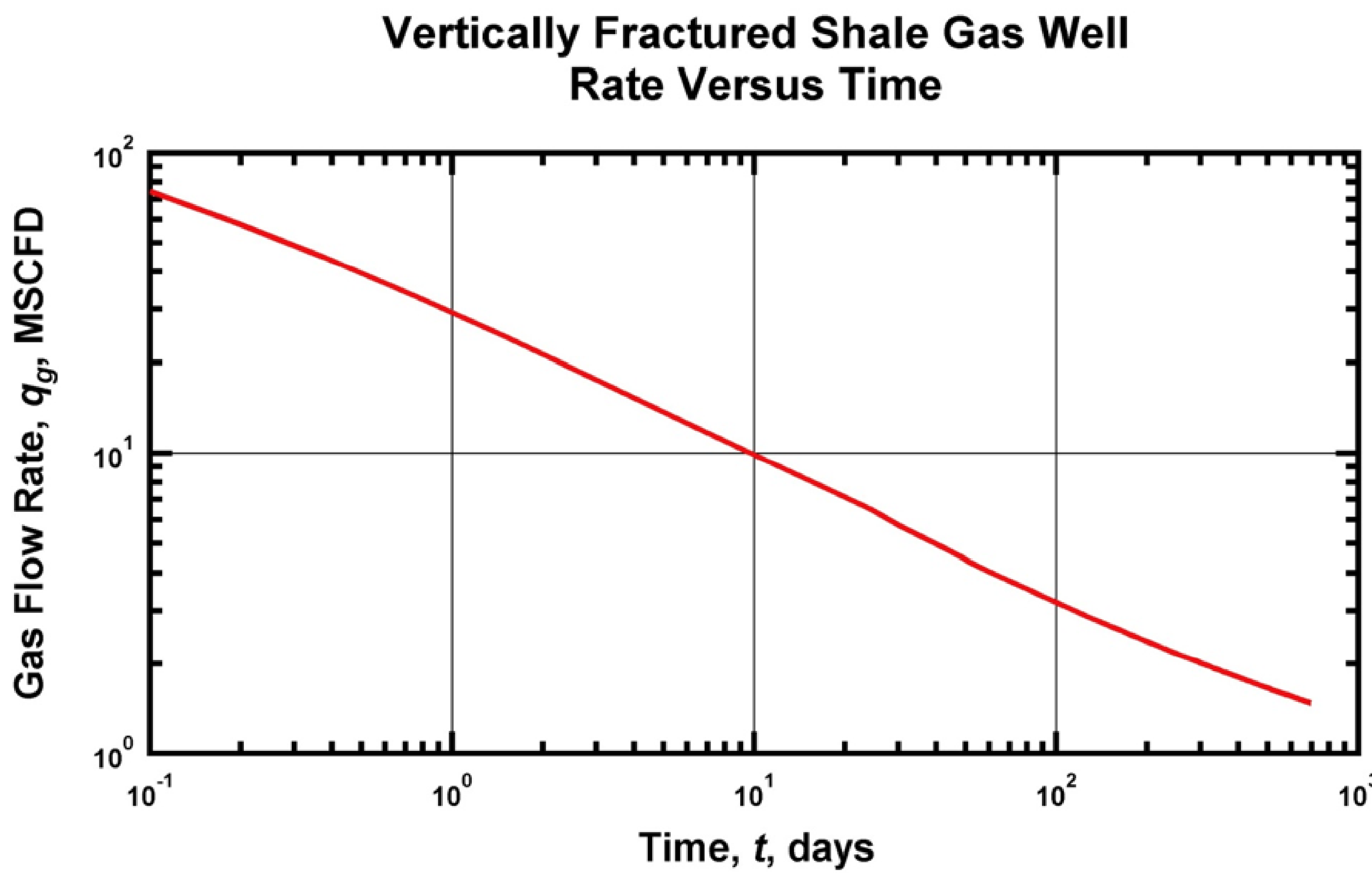

APPLICATION EXAMPLES

Problem A1: Gas production from a shale gas reservoir using a horizontal well

System Subdomains

- **S-1**: The original (undisturbed) rock system
  - Matrix
  - Possibly naturally fractured: Native fractures (NF)

APPLICATION EXAMPLES: Problem A1

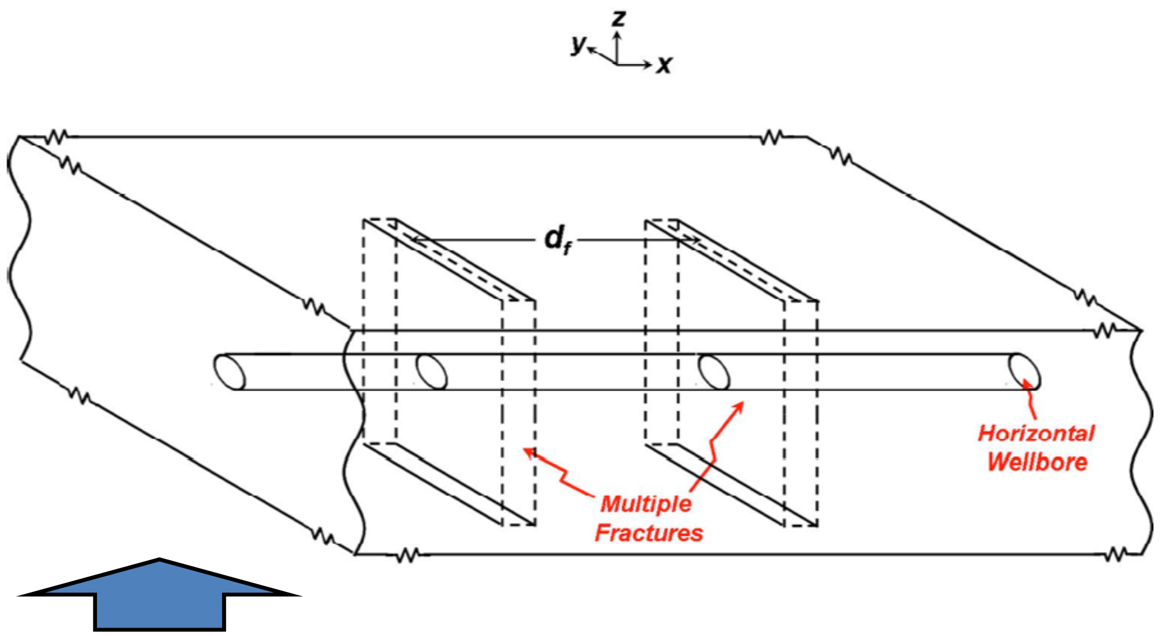

Well system, full schematic

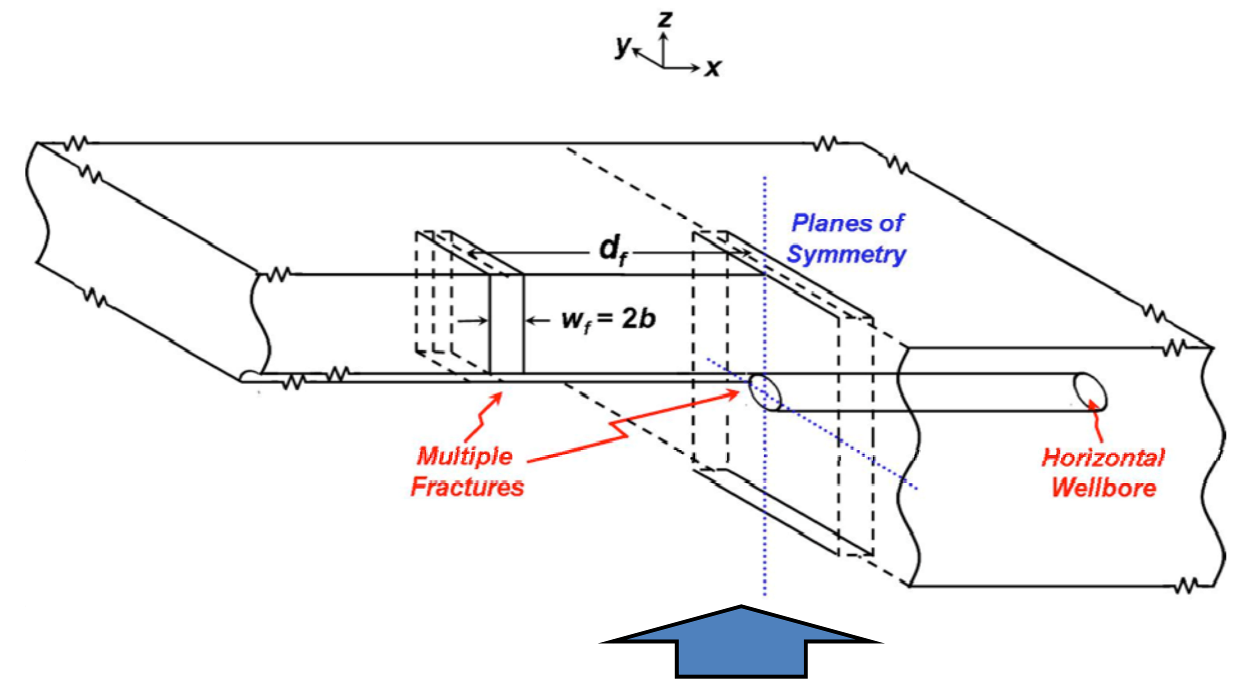

Symmetry argument

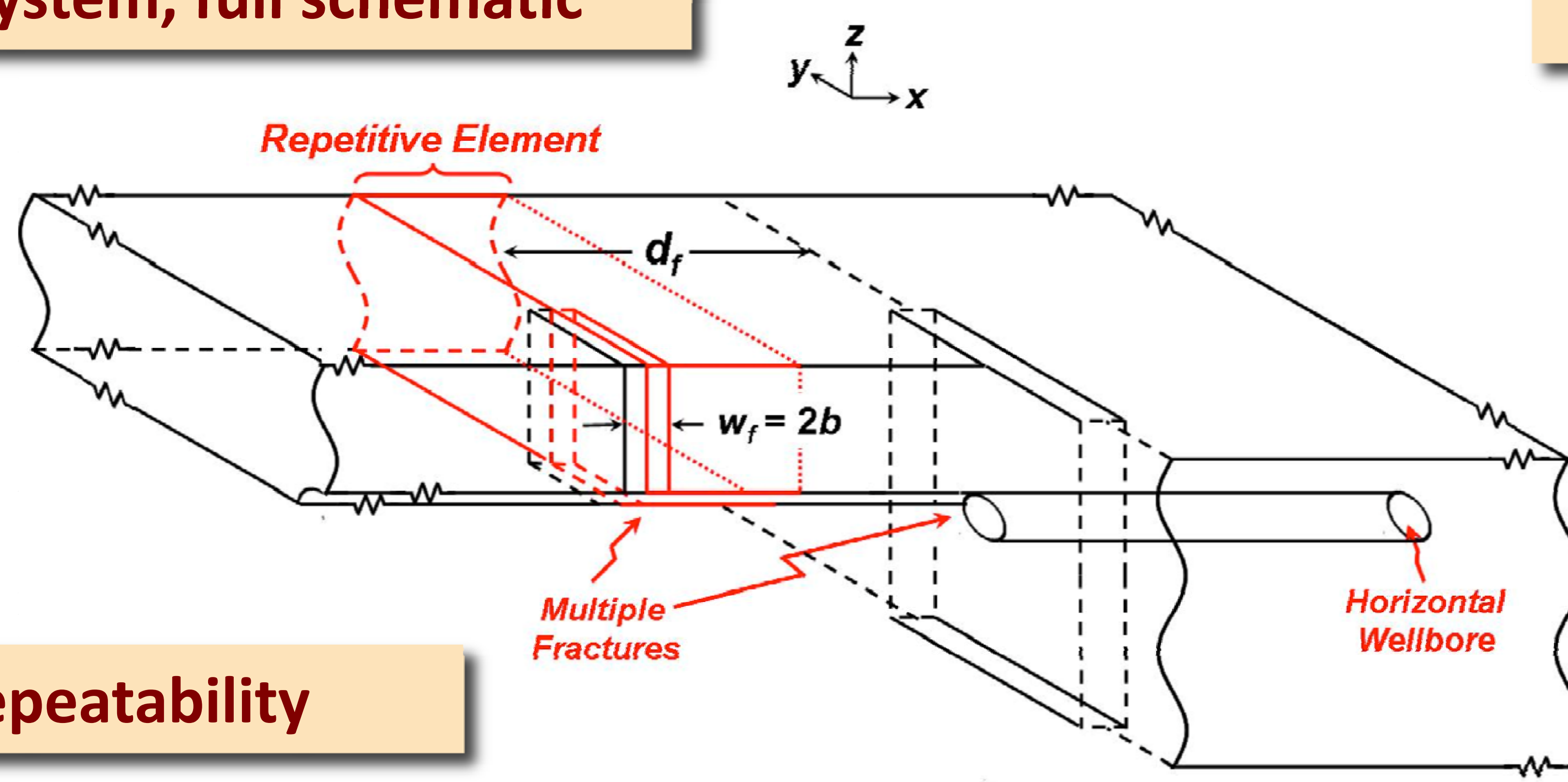

Computational element: Symmetry and repeatability (Freeman et al., 2009)

Repeatability

APPLICATION EXAMPLES: Problem A1

Important parameters

- d_{sr}: *thickness of stress-release fractured zone around wellbore*
- d_f: *primary fracture spacing*
- *b: primary fracture aperture*
- y_f: *y-reach of the primary fractures*
- L_y: *reservoir width*
- *h: reservoir thickness*

Similarly for vertical wells

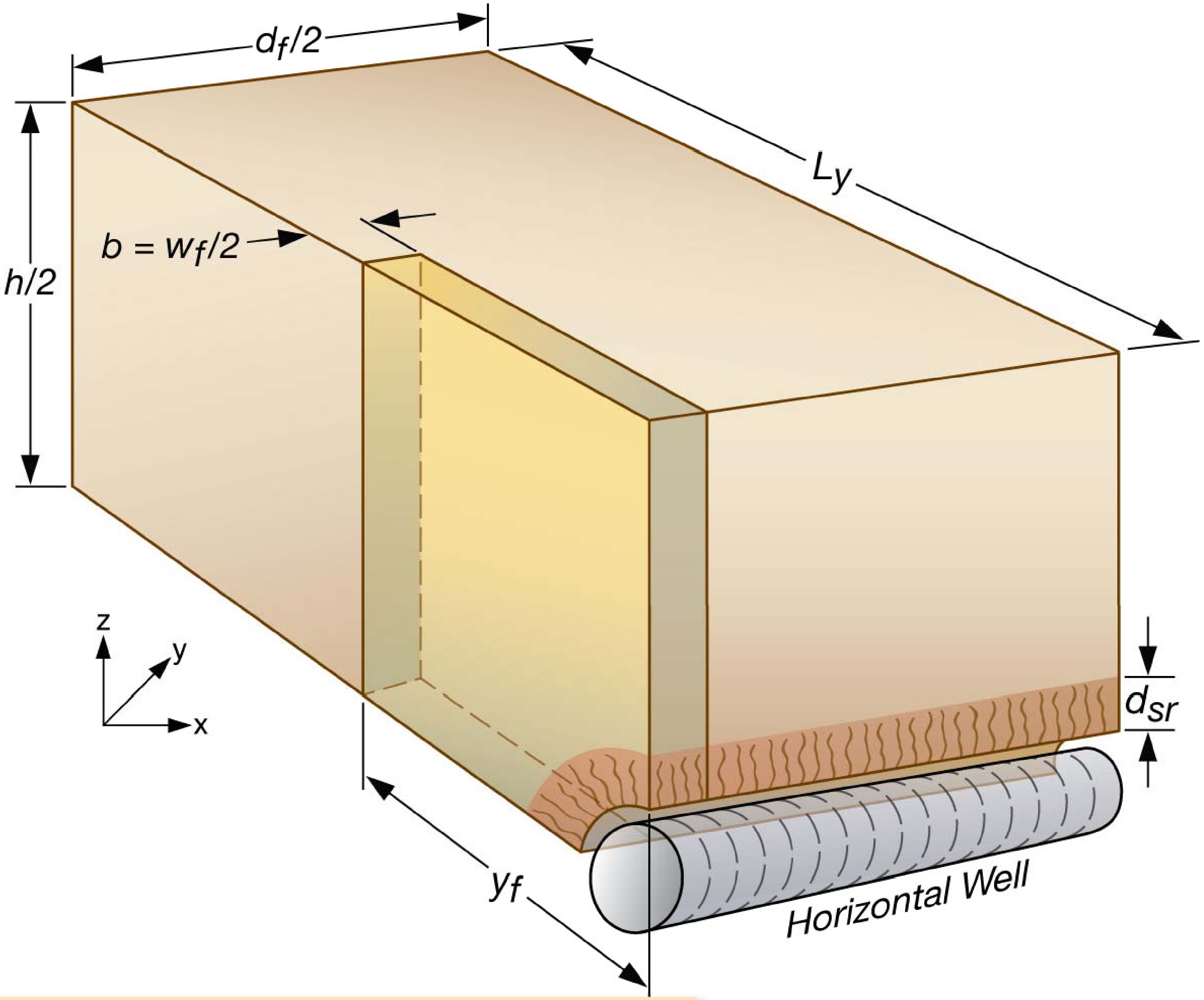

Type I: Reference

APPLICATION EXAMPLES: Problem A1

Numerical simulation results: 800,000 elements (Freeman, 2010; Moridis et al., 2010)

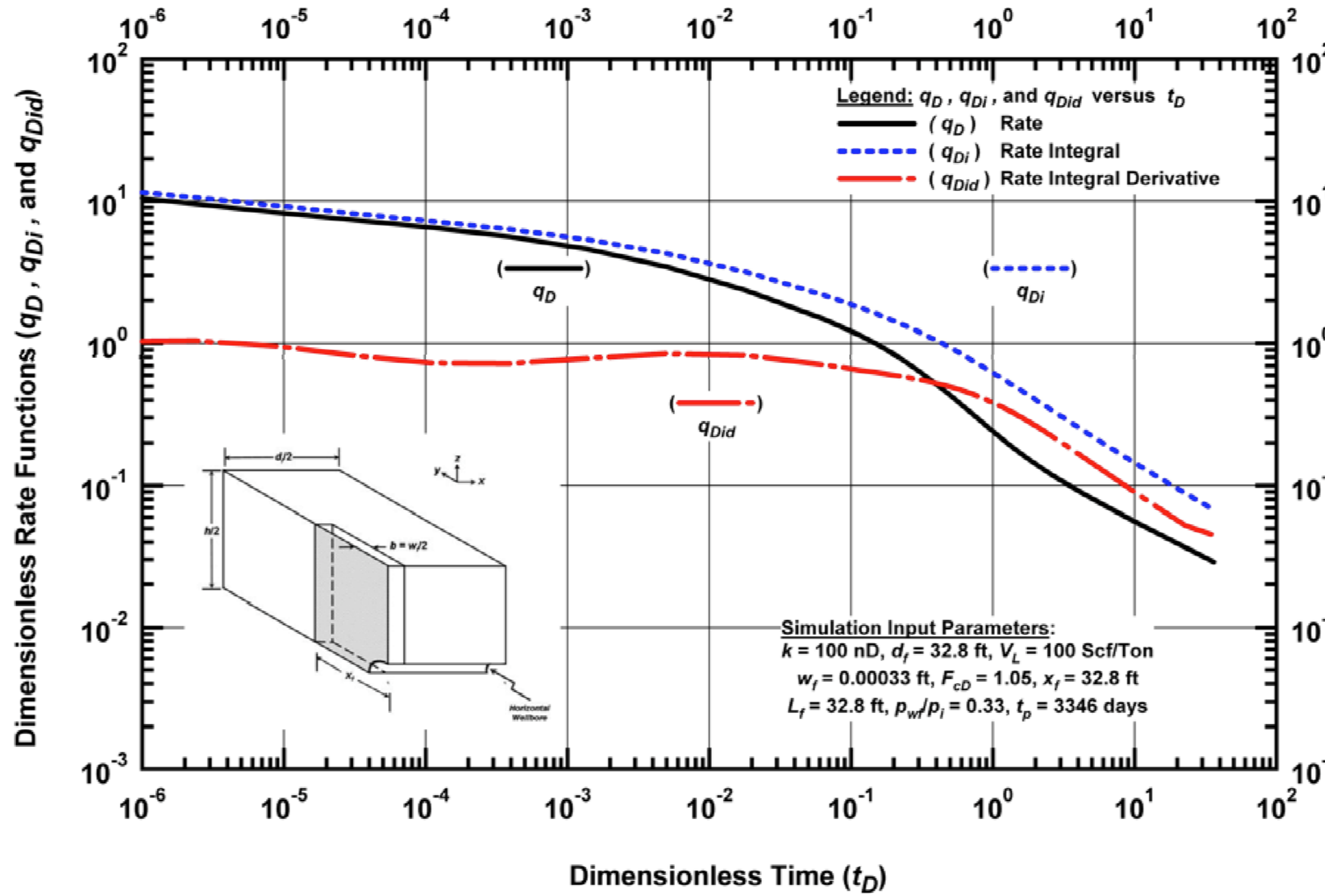

APPLICATION EXAMPLES: Problem A1

Numerical simulation results: 800,000 elements (Freeman, 2010; Moridis et al., 2010)

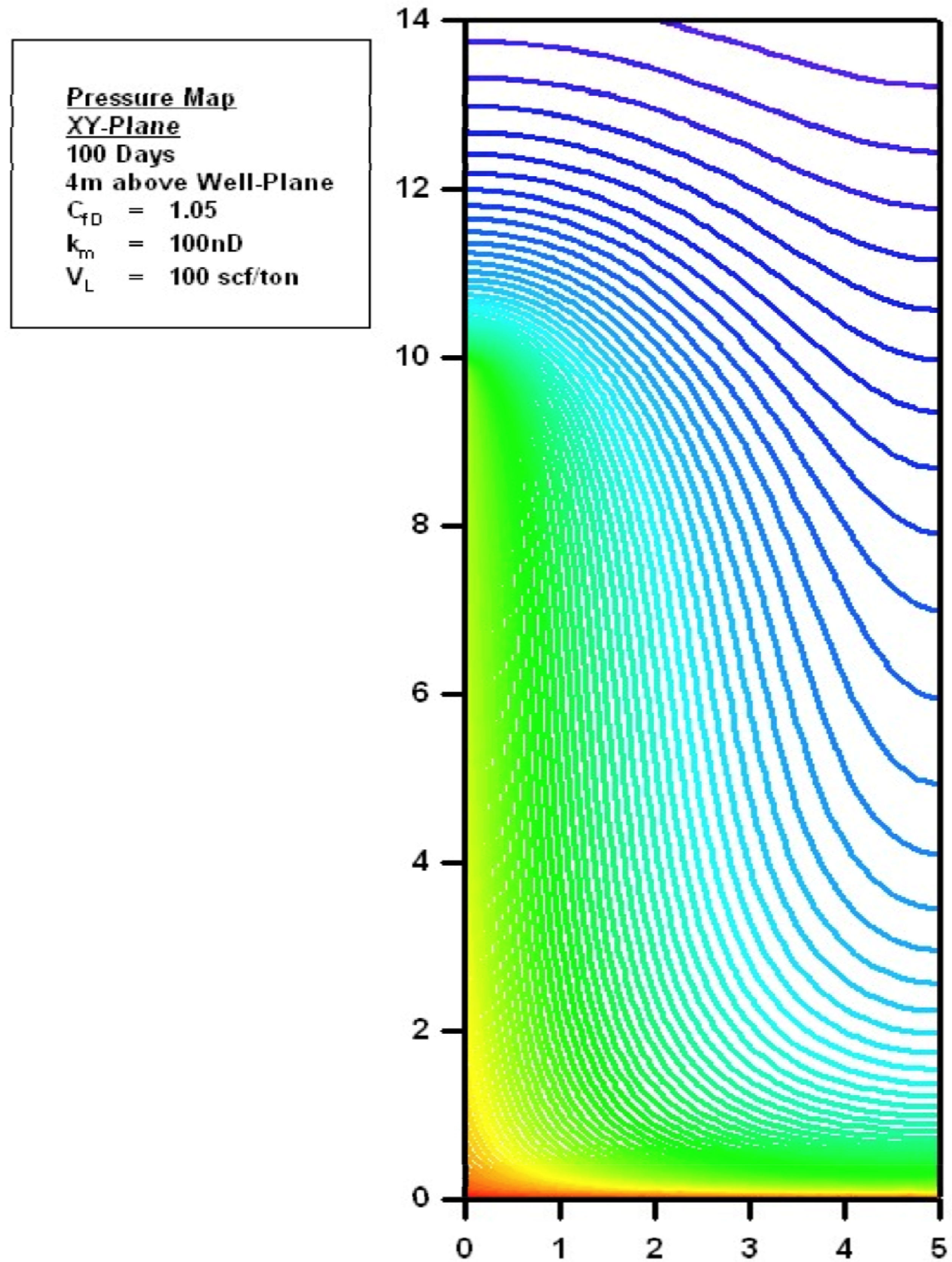

APPLICATION EXAMPLES: Problem A1

Sensitivity analyses (Freeman et al., 2011)

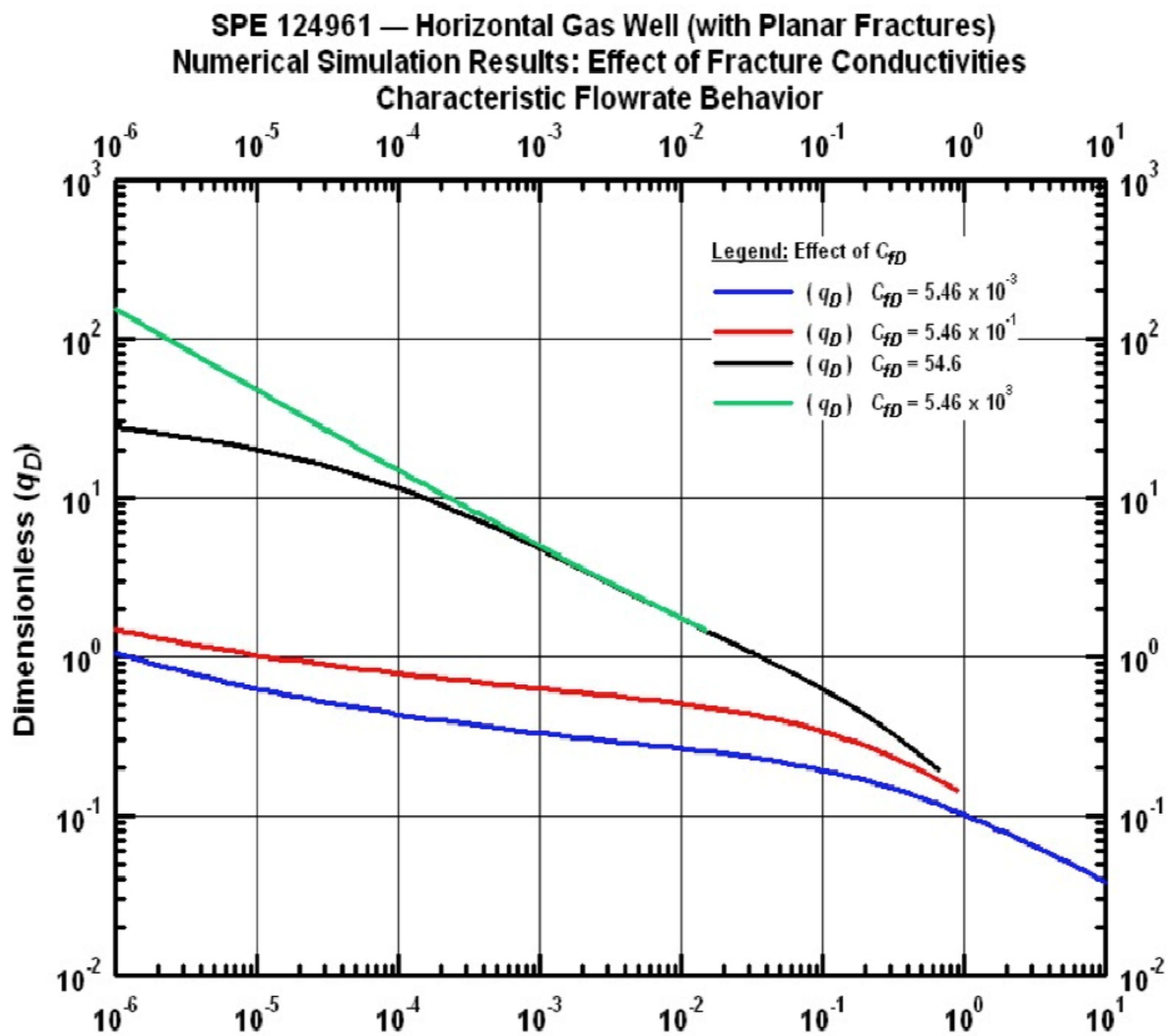

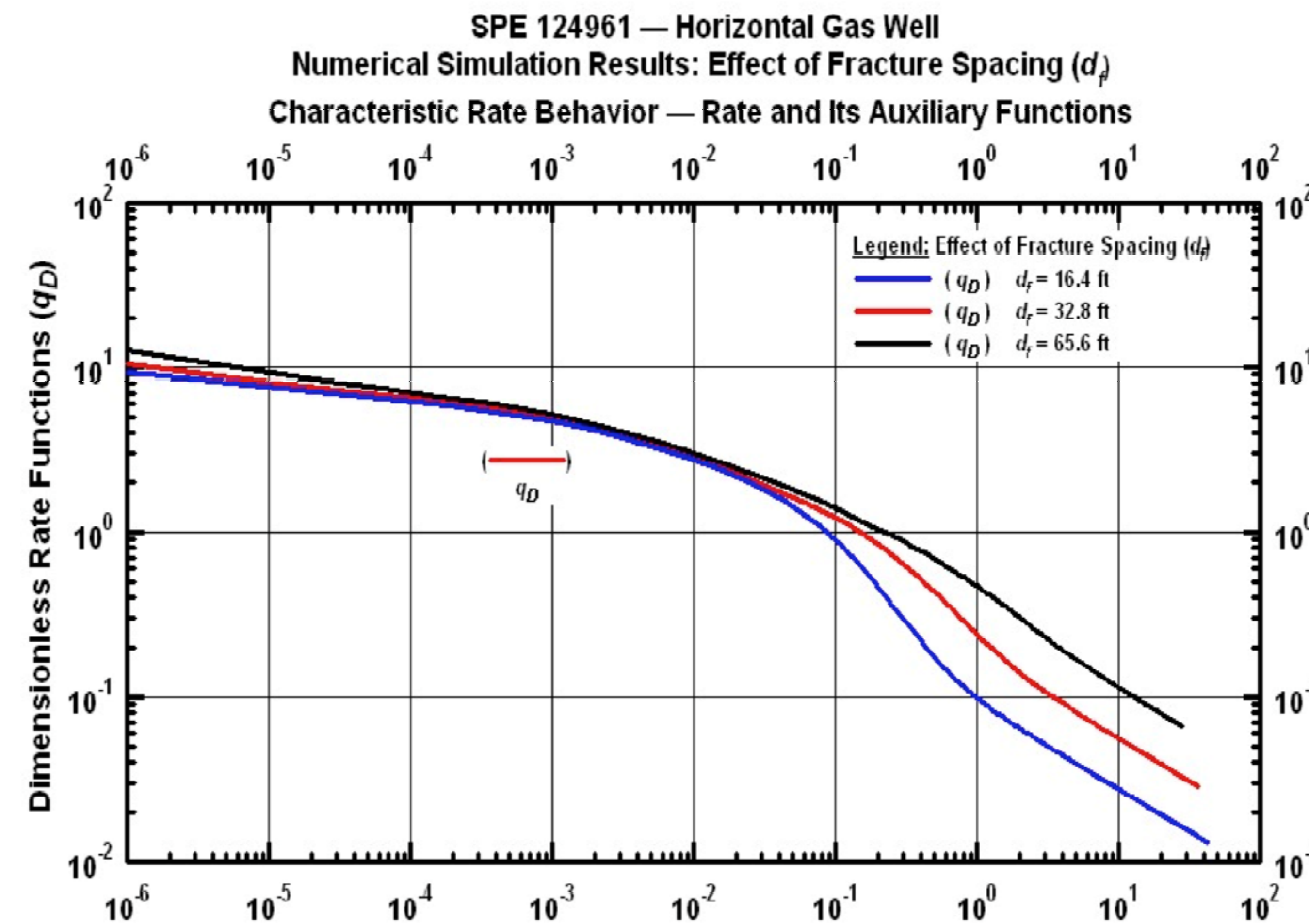

APPLICATION EXAMPLES

Problem A2: Gas production from a shale gas reservoir with a complex fracture system using a horizontal well

System Subdomains

- **S-1**: The original (undisturbed) rock system
  - Matrix
  - Possibly naturally fractured: Native fractures (NF)
- **S-2**: Fractures induced during stimulation: Primary fractures (PF)
  - Dominant pathways of flow to well
  - May intercept the NF system
- **S-3**: Stress-release fractures related to PF: Secondary fractures (SF)
  - Usually perpendicular to PF
  - Penetrate S-1, connected to PF, may intercept NF
- **S-4**: Stress-release fractures related to well drilling: Radial/tertiary fractures (RF/TF)
  - Usually cylindrical shape centered around the well axis
  - Connected to S-1 and PF, may intercept NF and SF

APPLICATION EXAMPLES: Problem A1

Type II: Stress-release planar fractures (secondary)

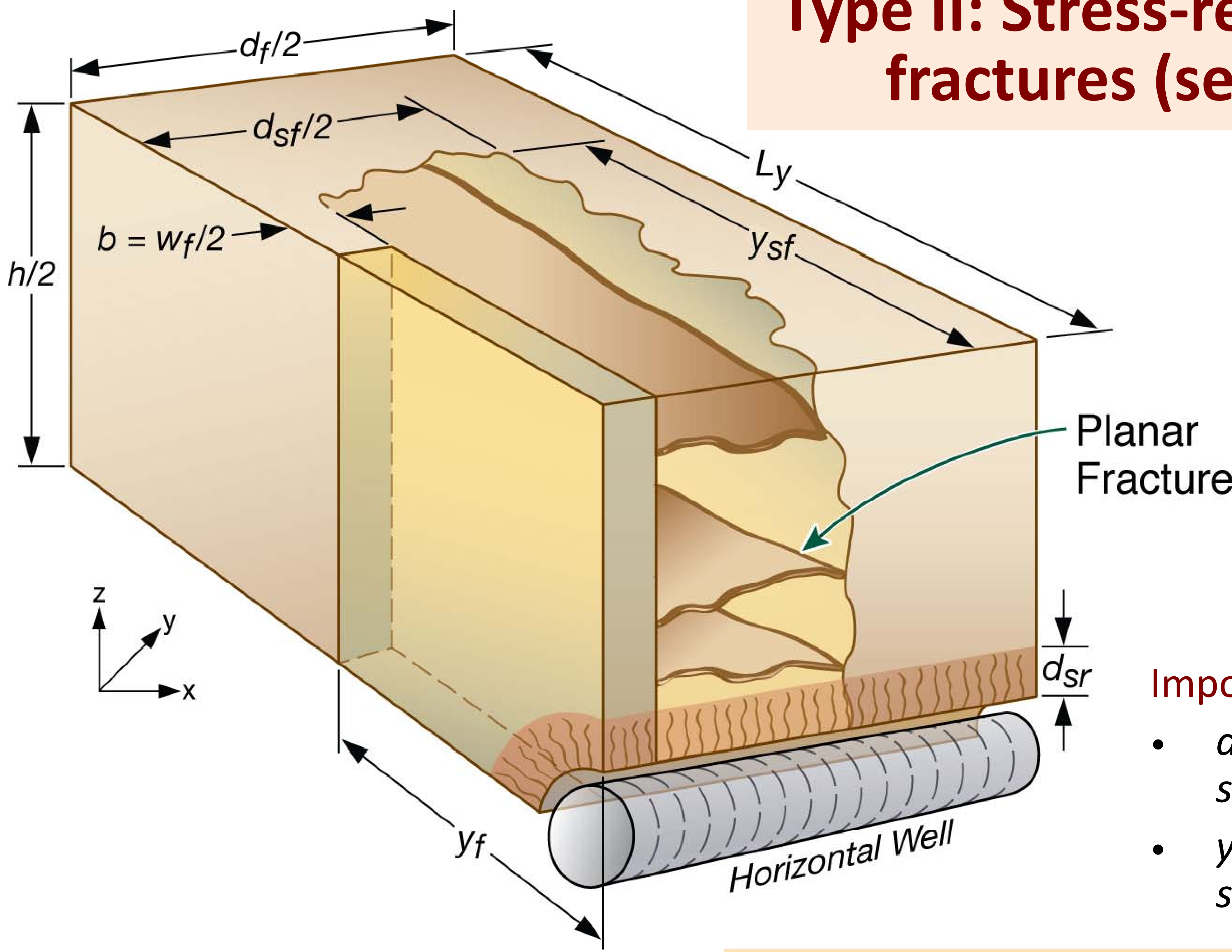

Important parameters

- d_{sf}: *x-reach of the secondary fractures*
- y_{sf}: *y-reach of the secondary fractures*

Similarly for vertical wells

APPLICATION EXAMPLES: Problem A2

Type III: Native & primary fractures

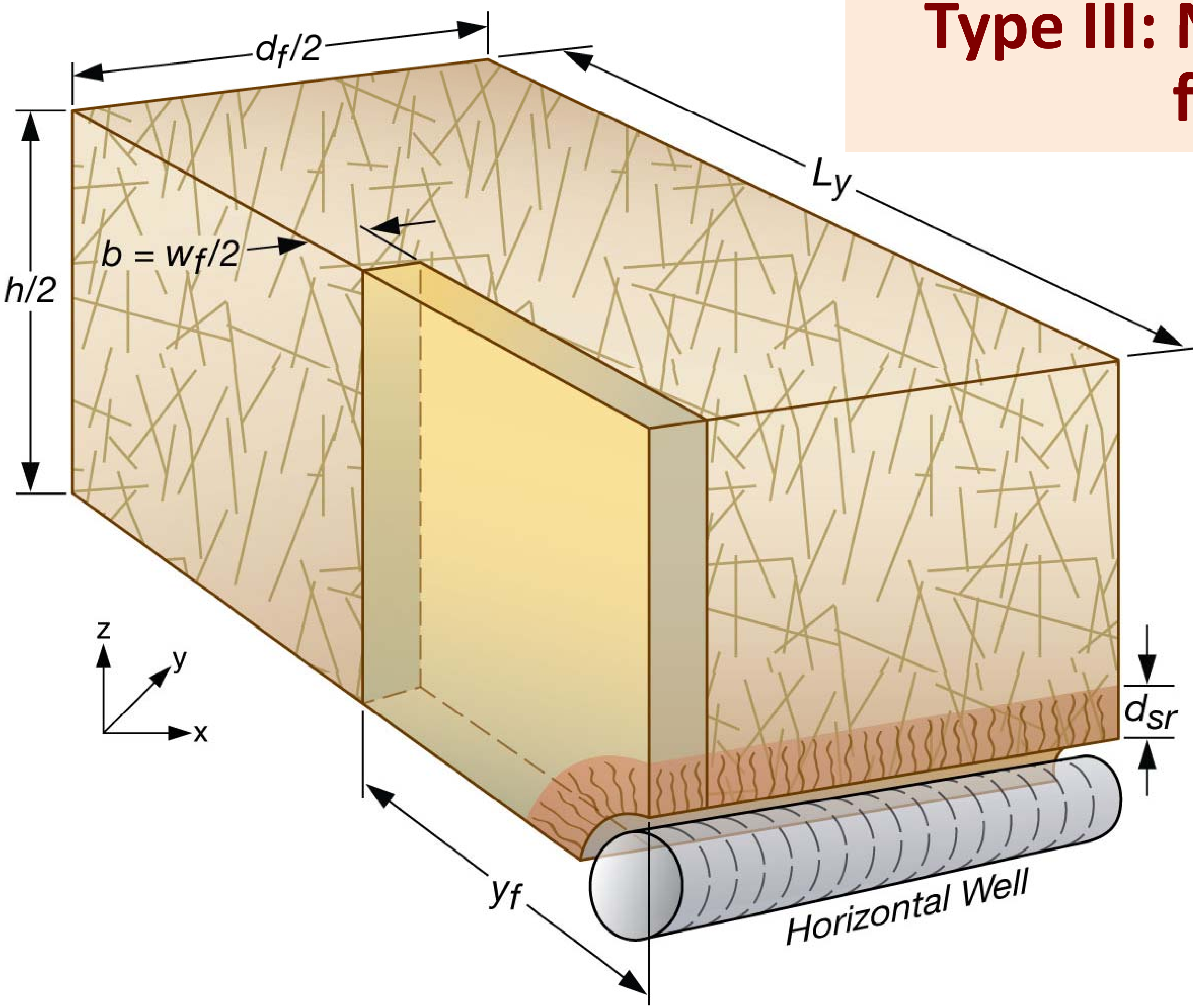

Similarly for vertical wells

Native fractures

- *Difficult to describe individually*

APPLICATION EXAMPLES: Problem A2

Type IV: All types of fractures

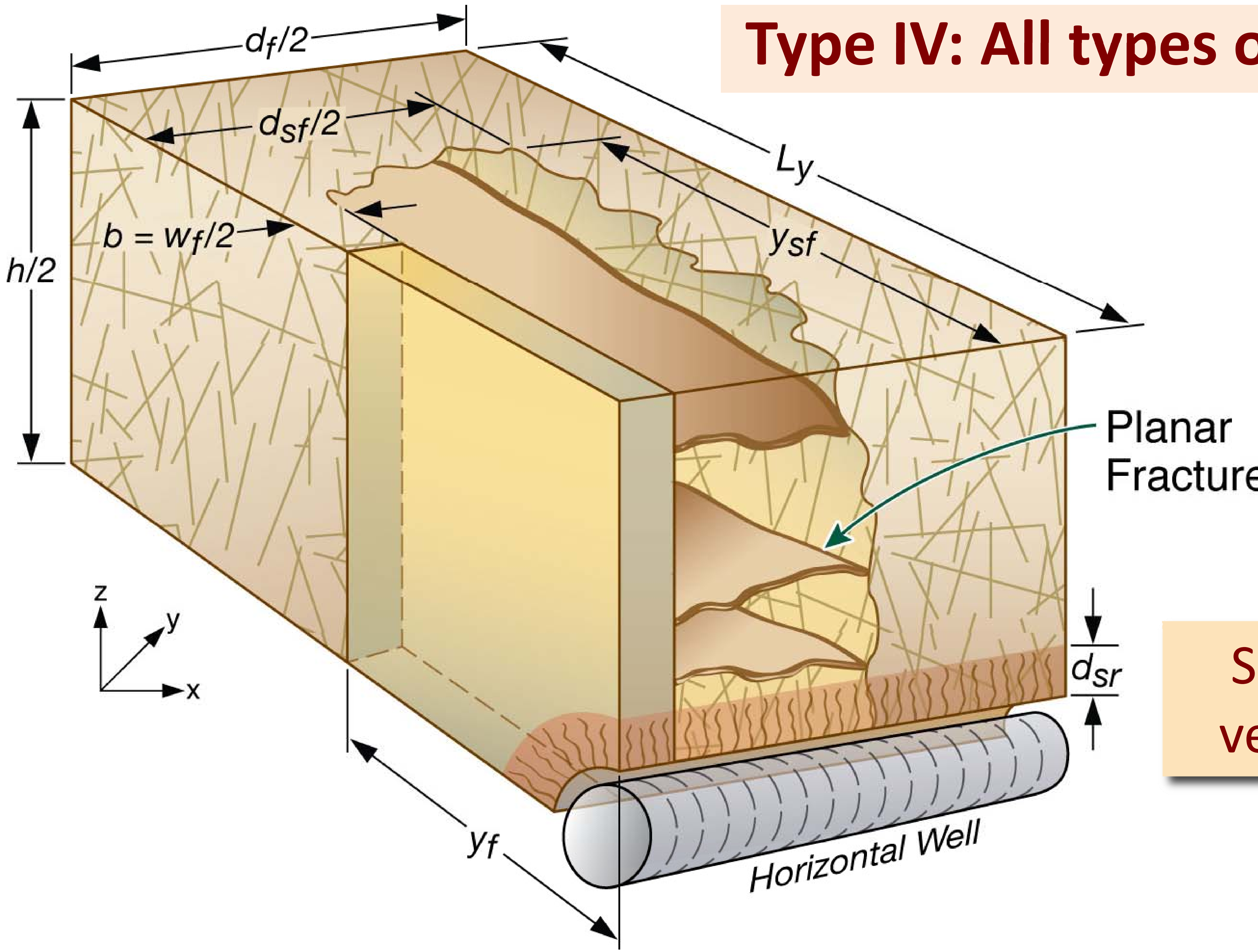

Similarly for vertical wells

APPLICATION EXAMPLES: Problem A2

Numerical simulation results: up to 1,200,000 elements (Freeman, 2010; Moridis et al., 2010)

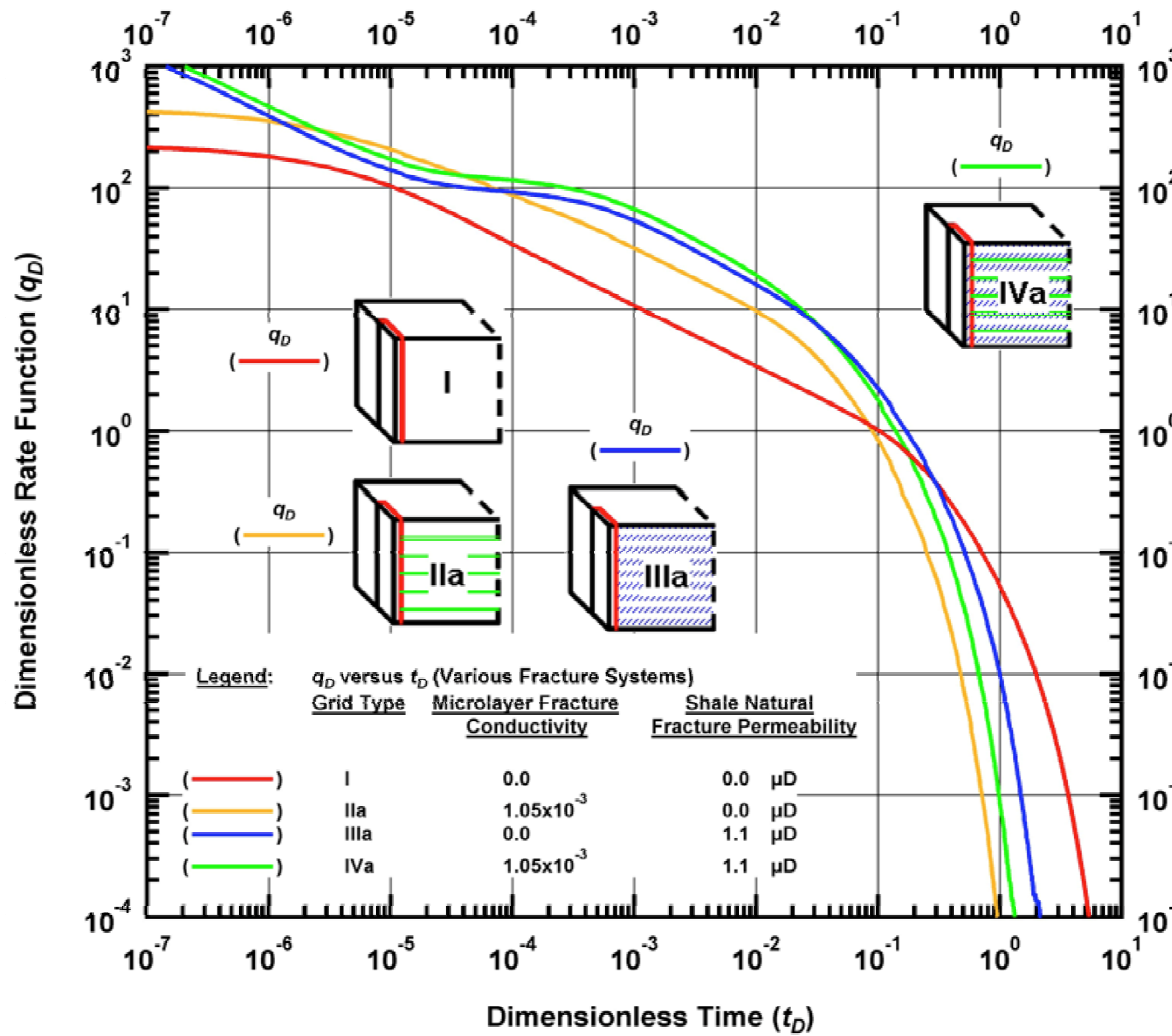

APPLICATION EXAMPLES

Problem A3: Flowing gas composition changes in shale gas wells

System Specifics: Type I

- Type I
- Gas Composition
  - $CH4$: 80%
  - C_2H_6 : 7%
  - C_3H_8 : 5%
  - C_4H_{10}: 5%
  - C_5H_{12}: 2%
  - C_6H_{16}: 1%

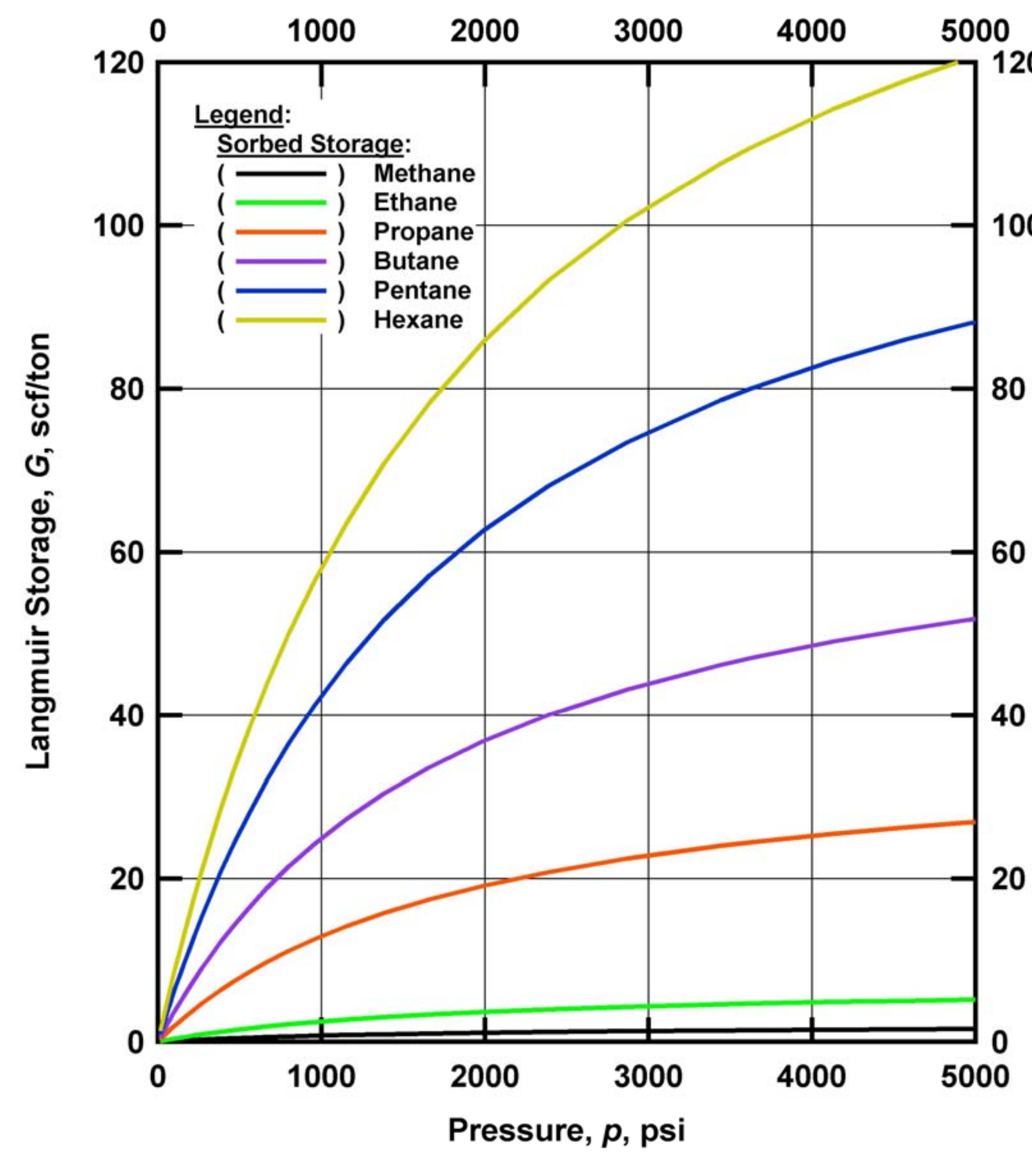

APPLICATION EXAMPLES: Problem A3

Numerical simulation results: 800,000 elements (Freeman et al., 2012)

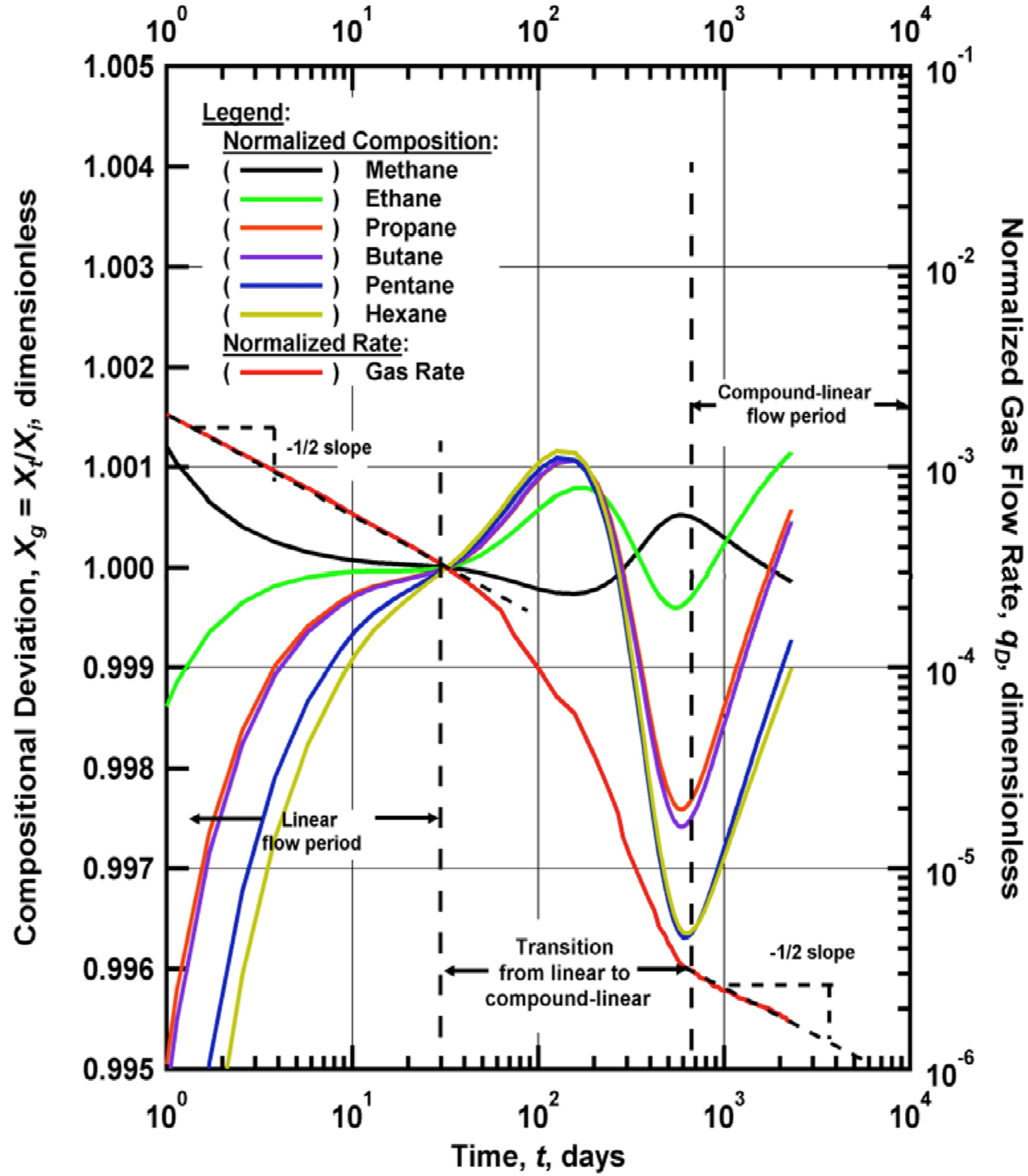

Modeling Failure Scenarios: Wells, Faults and Fractures

Artificial Pathways: Well(s)

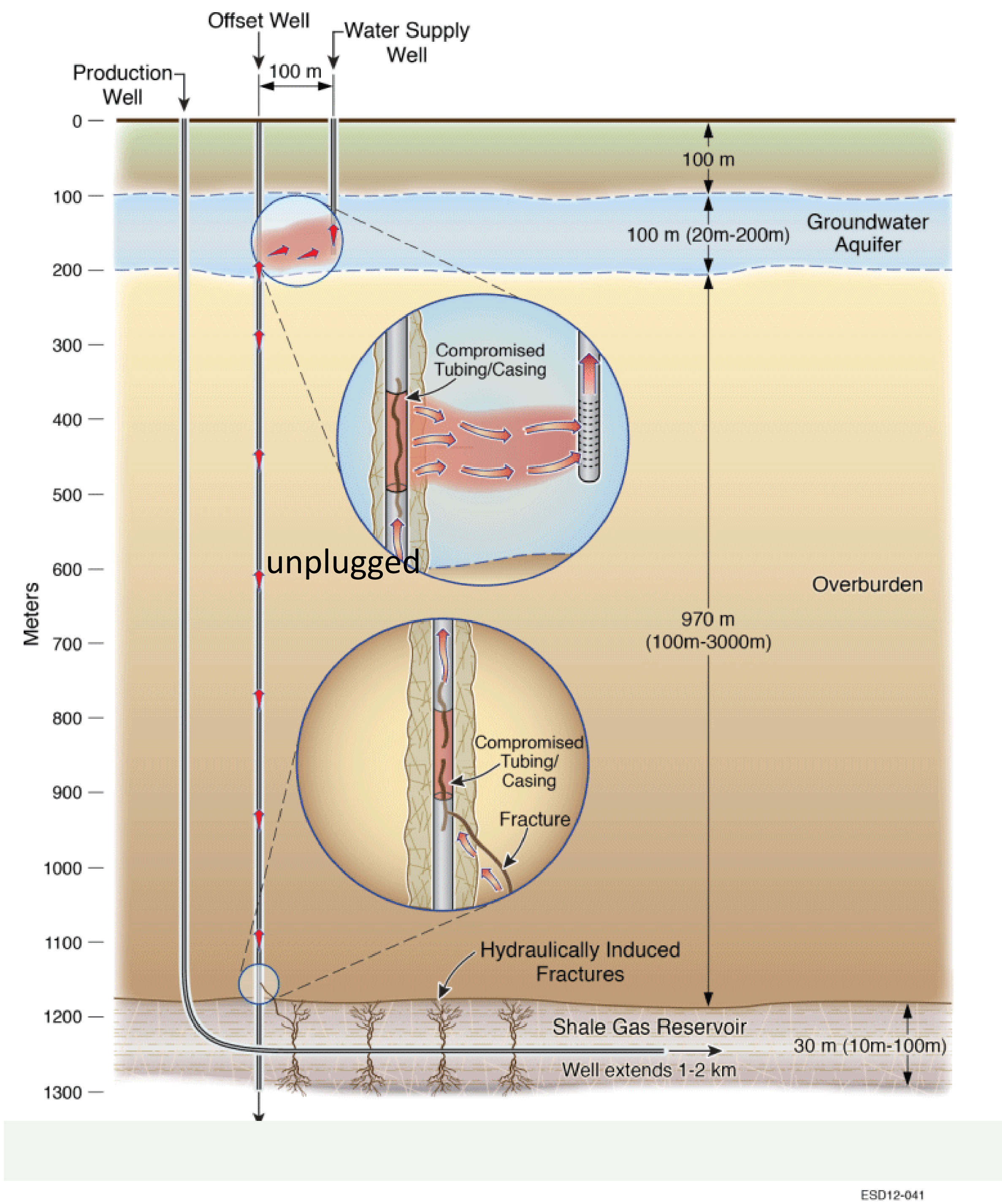

Natural Pathways: Faults or Fractures

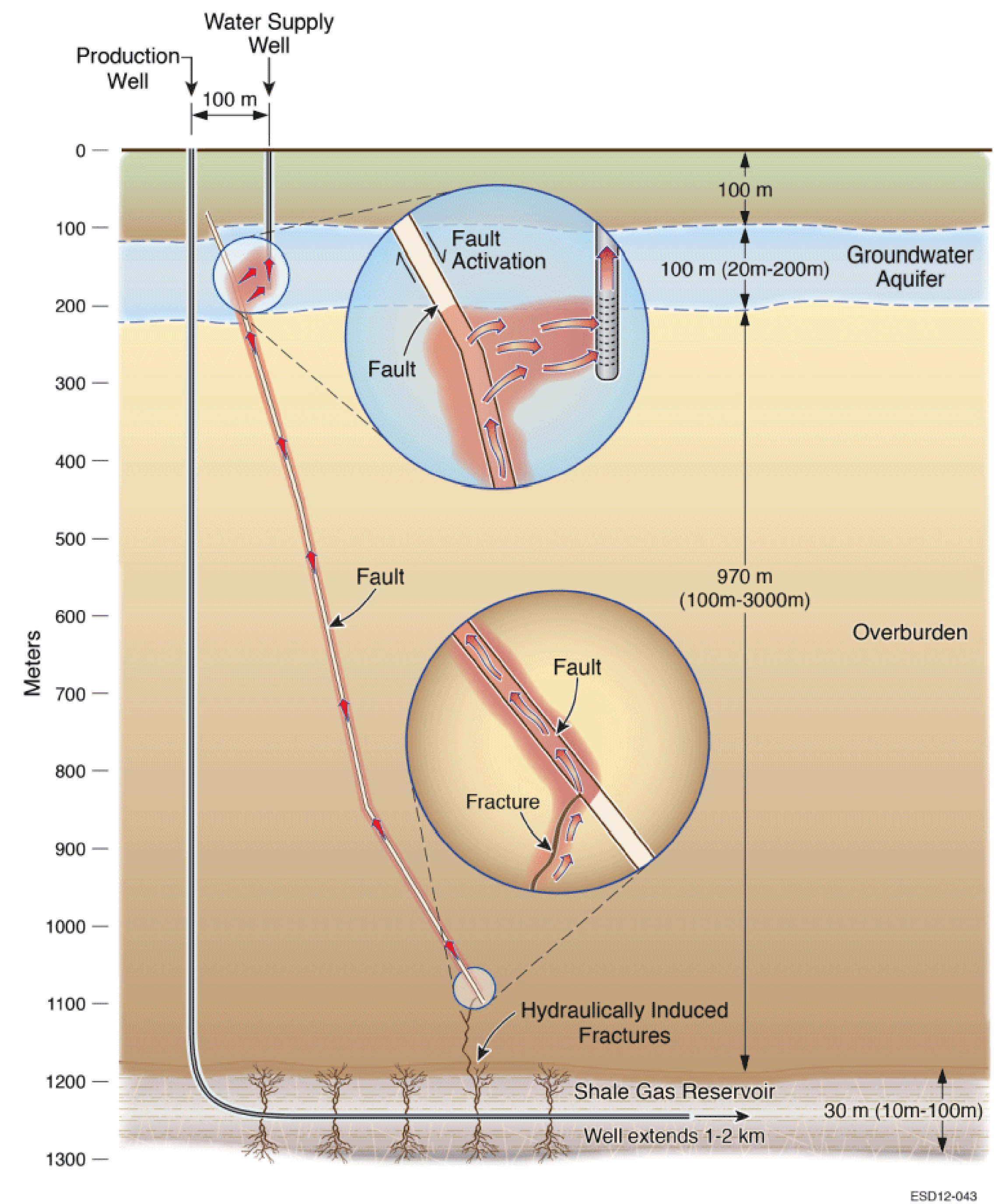

(1) Physically possible? **(2) Potential for fluid migration?**

Mesh Generation Process

MeshVoro code for unstructured mesh generation developed for complex 3D geometries.

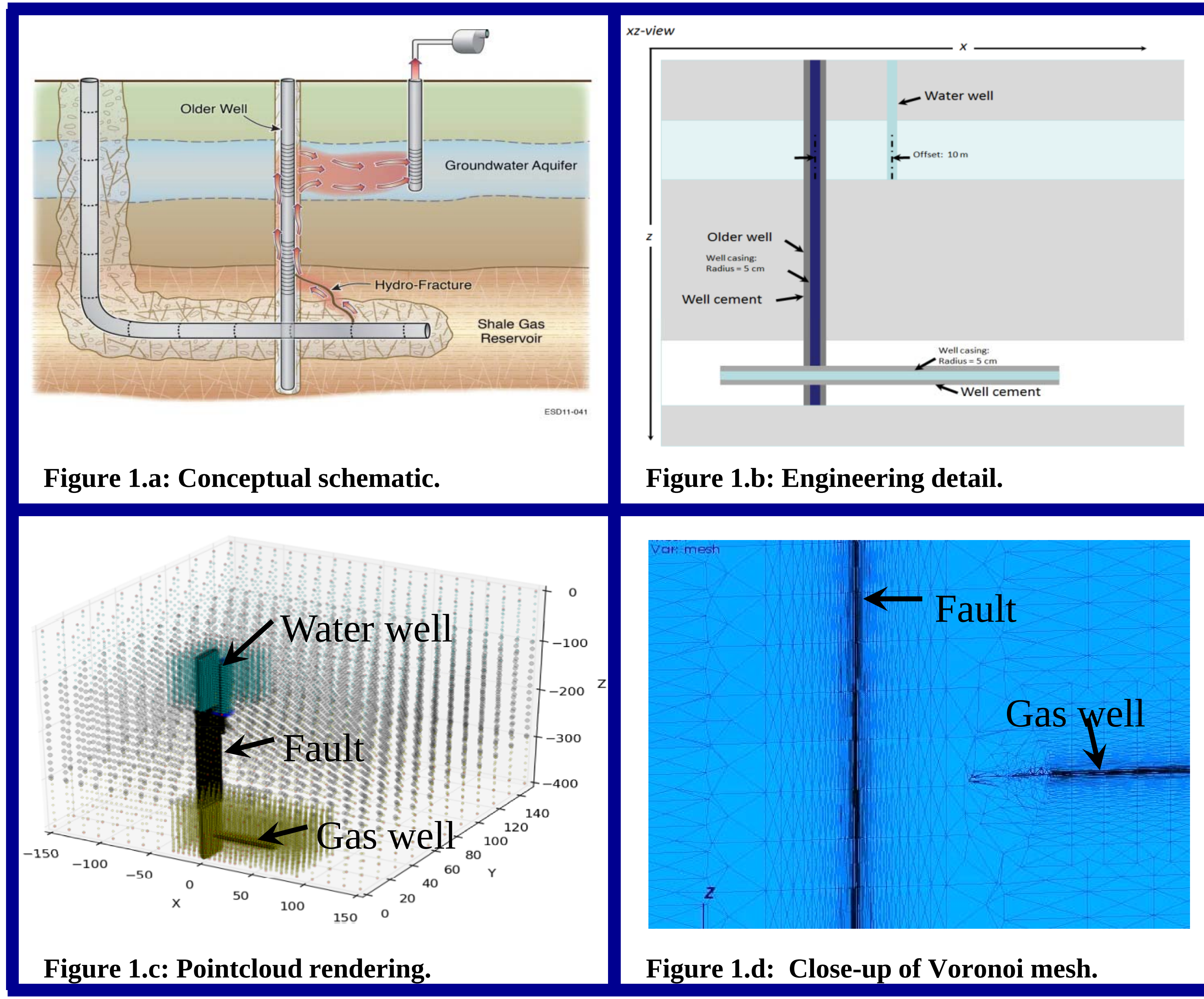

Figure 1.a: Conceptual schematic.

Figure 1.b: Engineering detail.

Figure 1.c: Pointcloud rendering.

Figure 1.d: Close-up of Voronoi mesh.

Workflow for generation of complex Voronoi meshes using the MeshVoro code base. The generated meshes typically possess between 100,000 and 500,000 elements.

Conceptual Model Building:

Scenarios: Well(s) as a Pathway

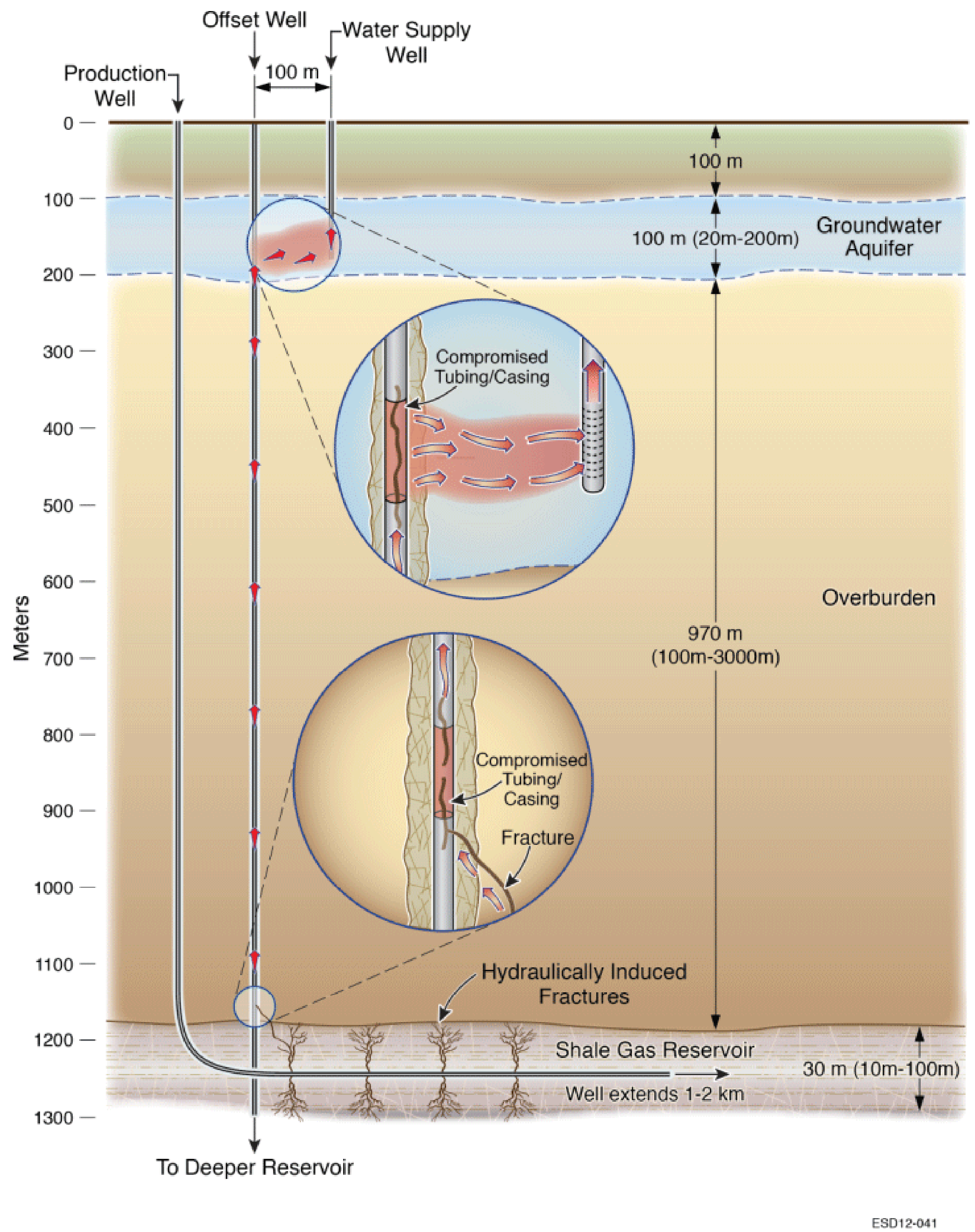

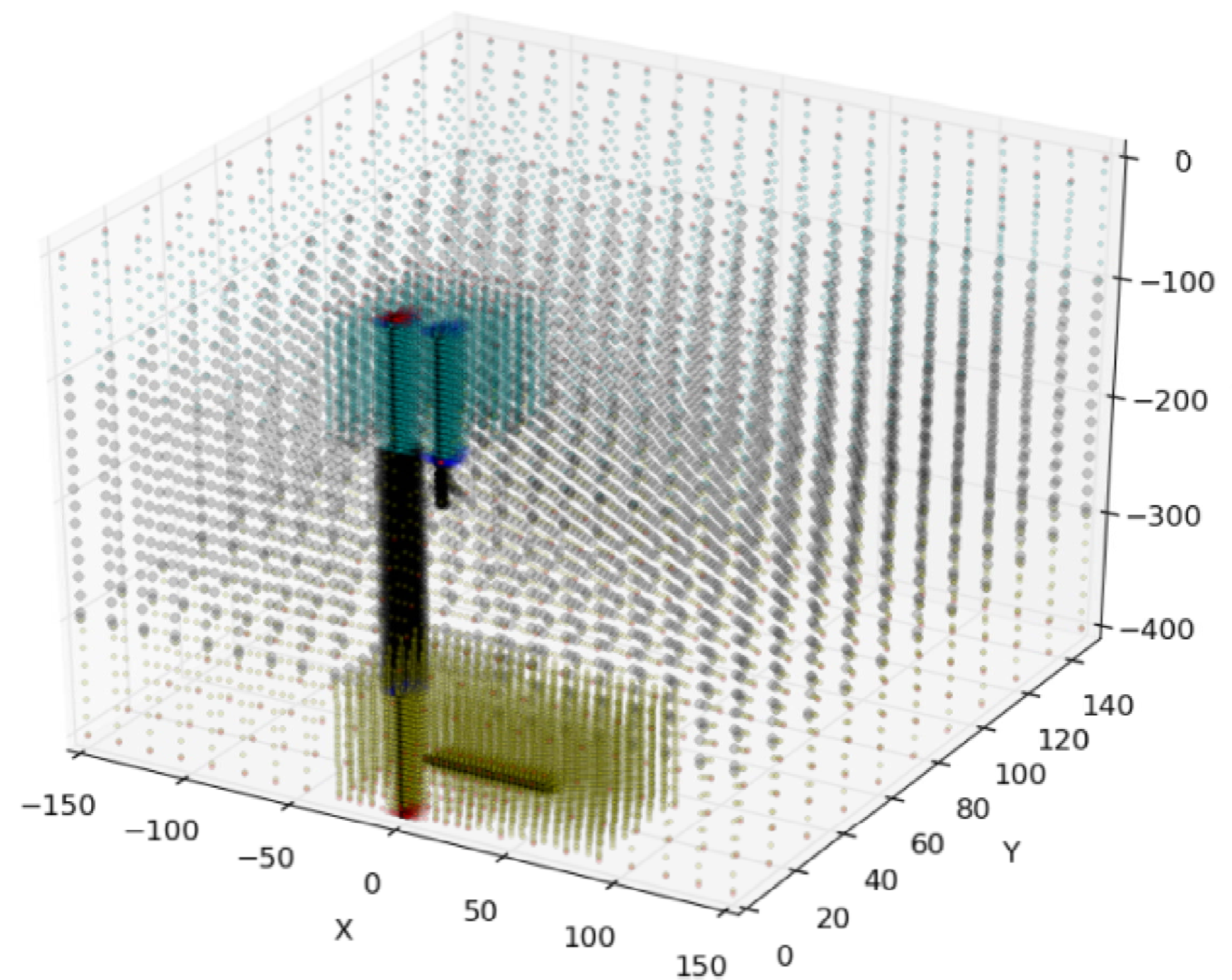

Various zones of the simulated system. Colors denote different material types.

Conceptual Model Building:

Scenarios: Fault/Fractures Pathway

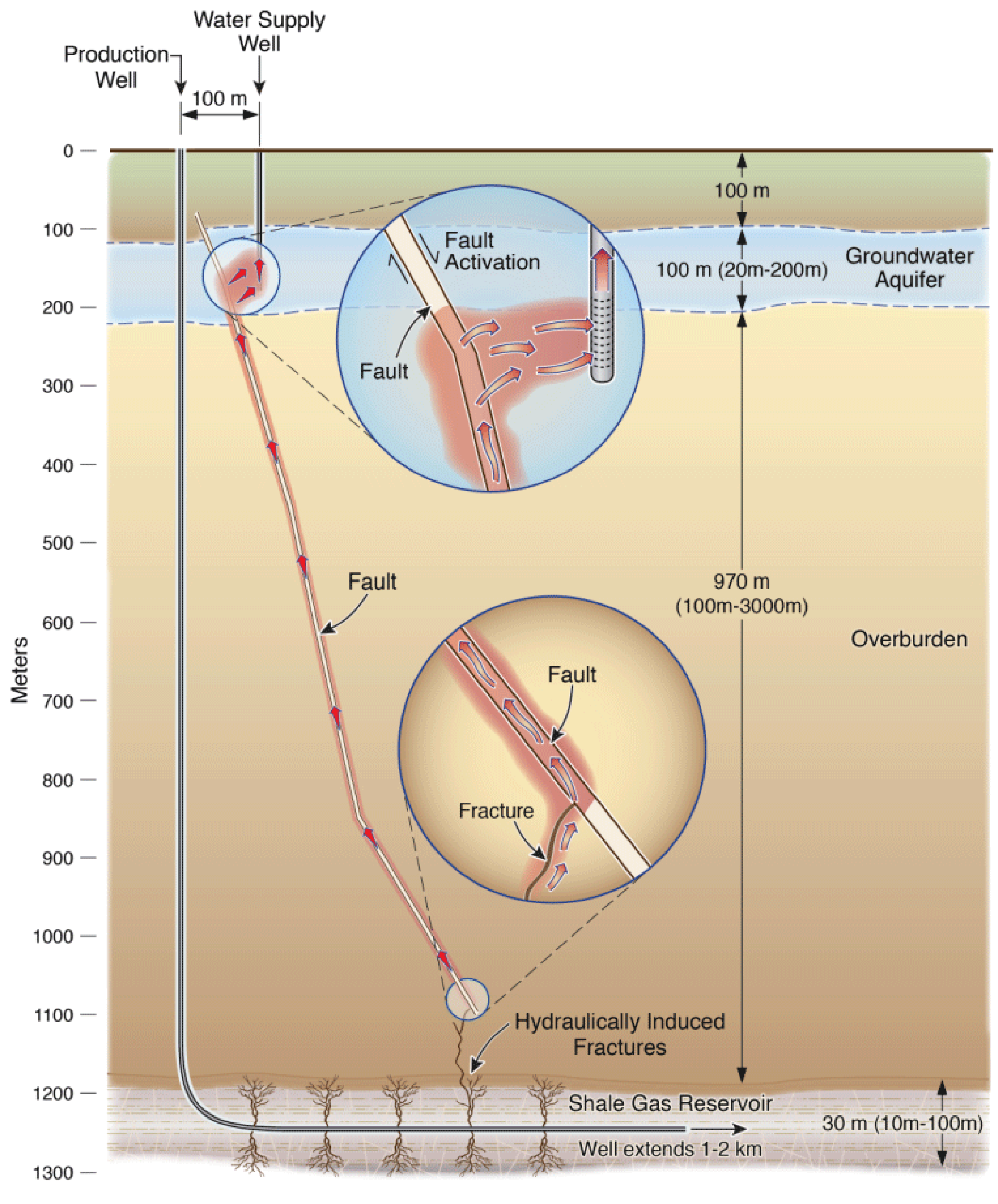

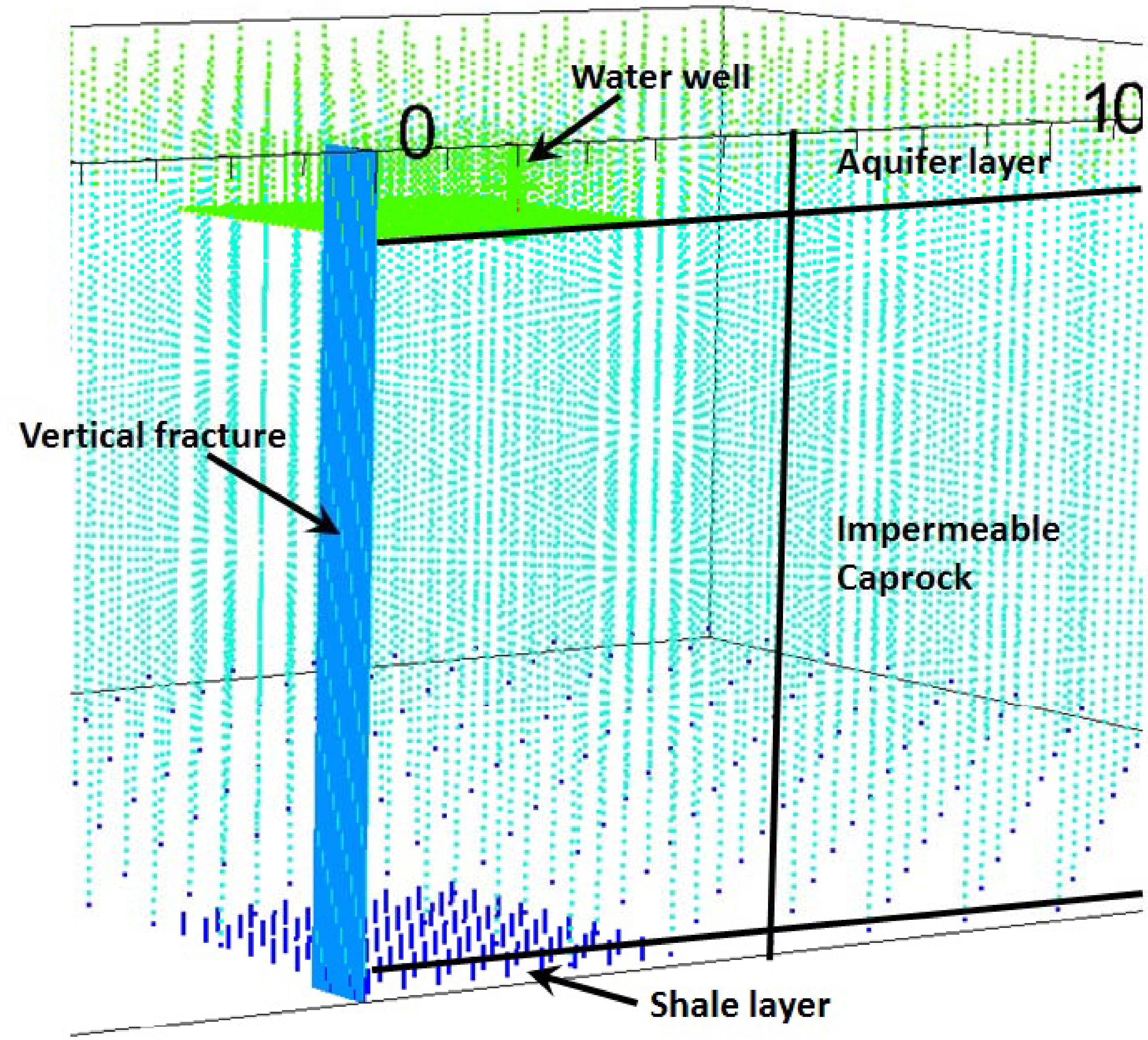

Annotated view of the various zones of the simulated system. Colors denote different material types.

Some properties & conditions of systems under investigation

Abandoned leaking well

k_{shale} (m^2)	k_{well} (m^2)	Well Production Rates: Shale well (kg/s)	Well Production Rates: Water well (gpm)
3.00E-19	3.00E-09	**1.00E-03**	0.00E+00
3.00E-19	3.00E-09	**1.00E-04**	**1.00E-01**
3.00E-19	**3.00E-14**	0.00E+00	0.00E+00
3.00E-18	**3.00E-14**	0.00E+00	0.00E+00

Penetrating fracture

k_{shale} (m^2)	k_{frac} (m^2)	Shale well (kg/s)	Water well (gpm)
3.00E-18	3.00E-13	0.00E+00	0.00E+00
3.00E-19	3.00E-13	0.00E+00	0.00E+00

Partial lists

Sensitivity Analysis:

Characterize the problem space

1) Sensitivity parameters:
   - Conductivity of the leaking pathway (well/fault/fracture)
   - Production rate from **water** well
   - Production rate from **shale** well
   - Permeability of the shale
   - Vertical distance between gas-bearing shale and aquifer
   - Relative pressure regimes between the aquifer and the shale (as affected by respective production rates)

Results:

Gas plume rises through fracture

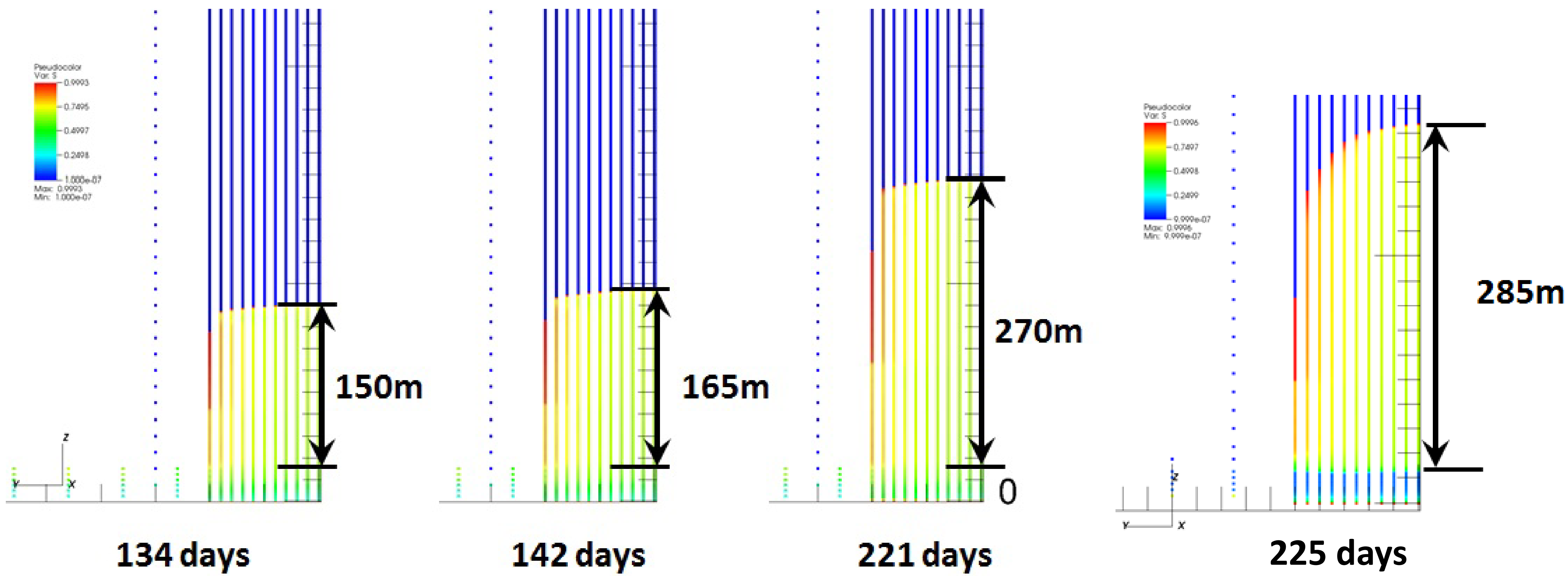

Saturation distribution at along the fracture at time snapshots of 134 days, 142 days, 221 days, and 225 days depicting the behavior of the gas plume over time with an overlying water well providing suction.

Results:

Gas plume rises through wellbore

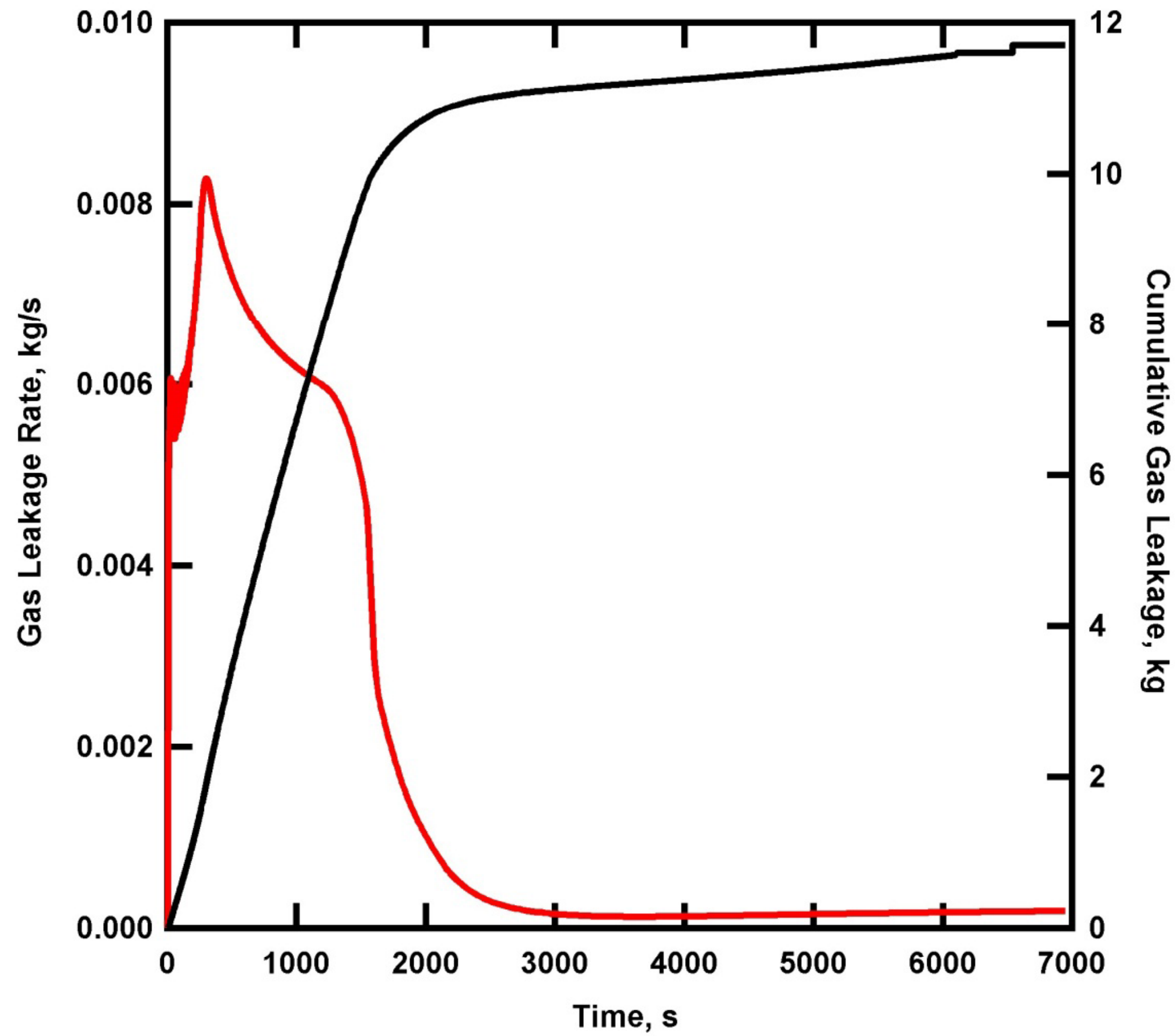

Gas leakage rate and cumulative leaked gas through an old abandoned well, with a shale layer permeability of 3.0e-18 m^2 and a wellbore permeability of 3.0e-9 m^2. After an initial "bubble" of gas (~11 kg) percolates to the aquifer, the leakage rate drops to approximately 2.2e-4 kg, or 19.0 kg/day, and then rises very gradually.

Results:
Drawdown of aquifer

a.

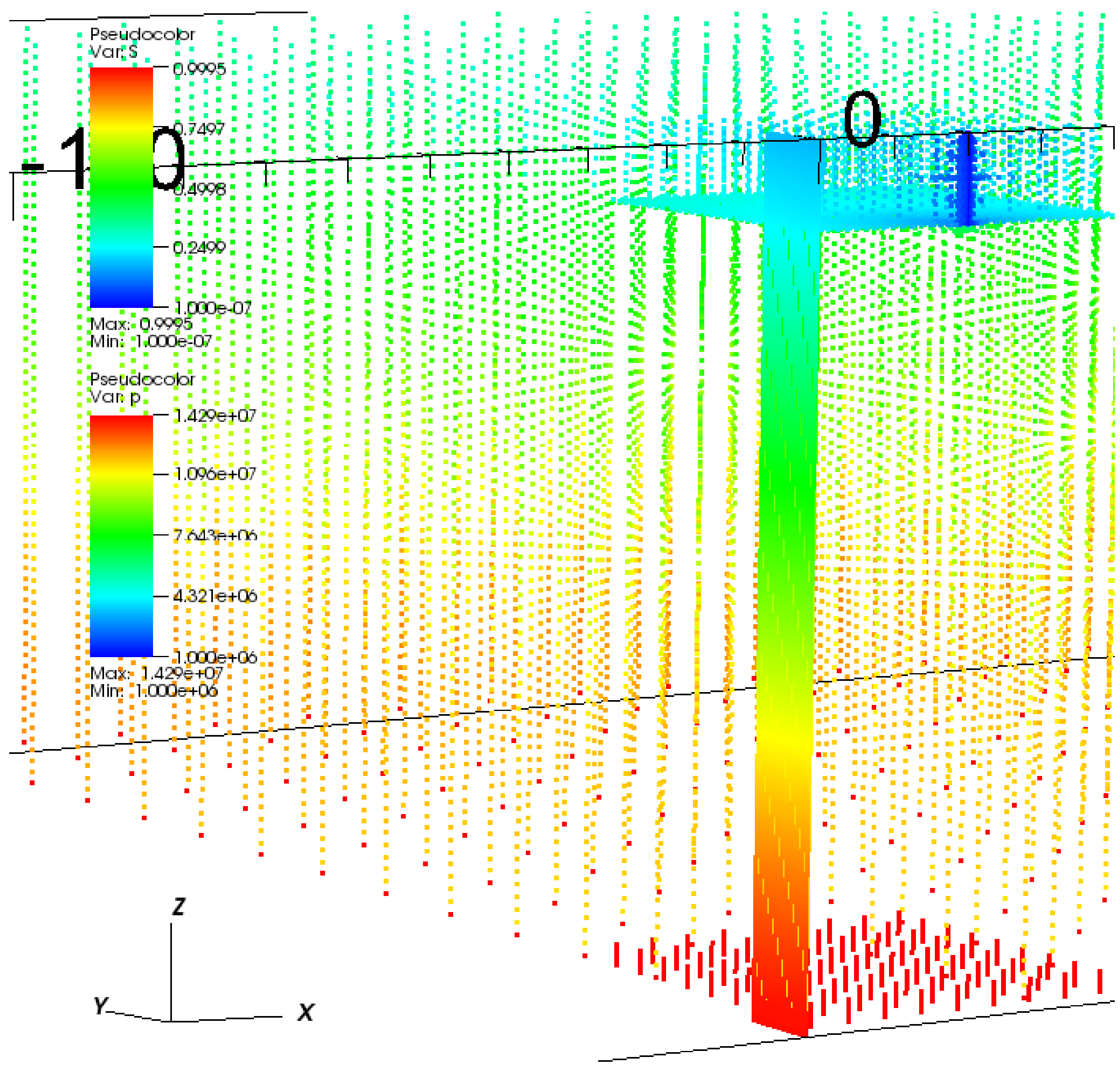

b.

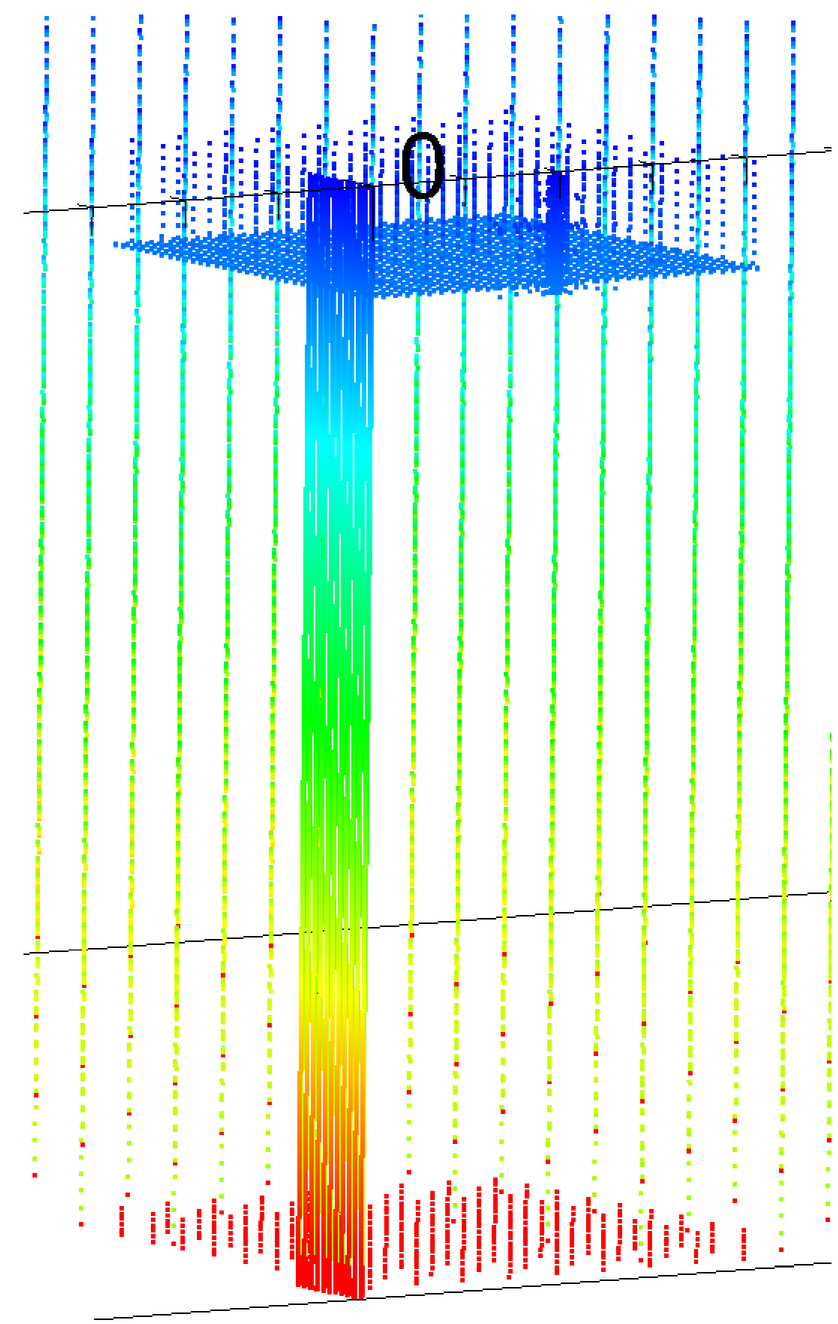

a. Pressure distribution at 134 days with water well producing at 1.0e6 Pa bottomhole pressure;
b. Pressure distribution at 221 days with water well producing at 1.0e6 Pa bottomhole pressure

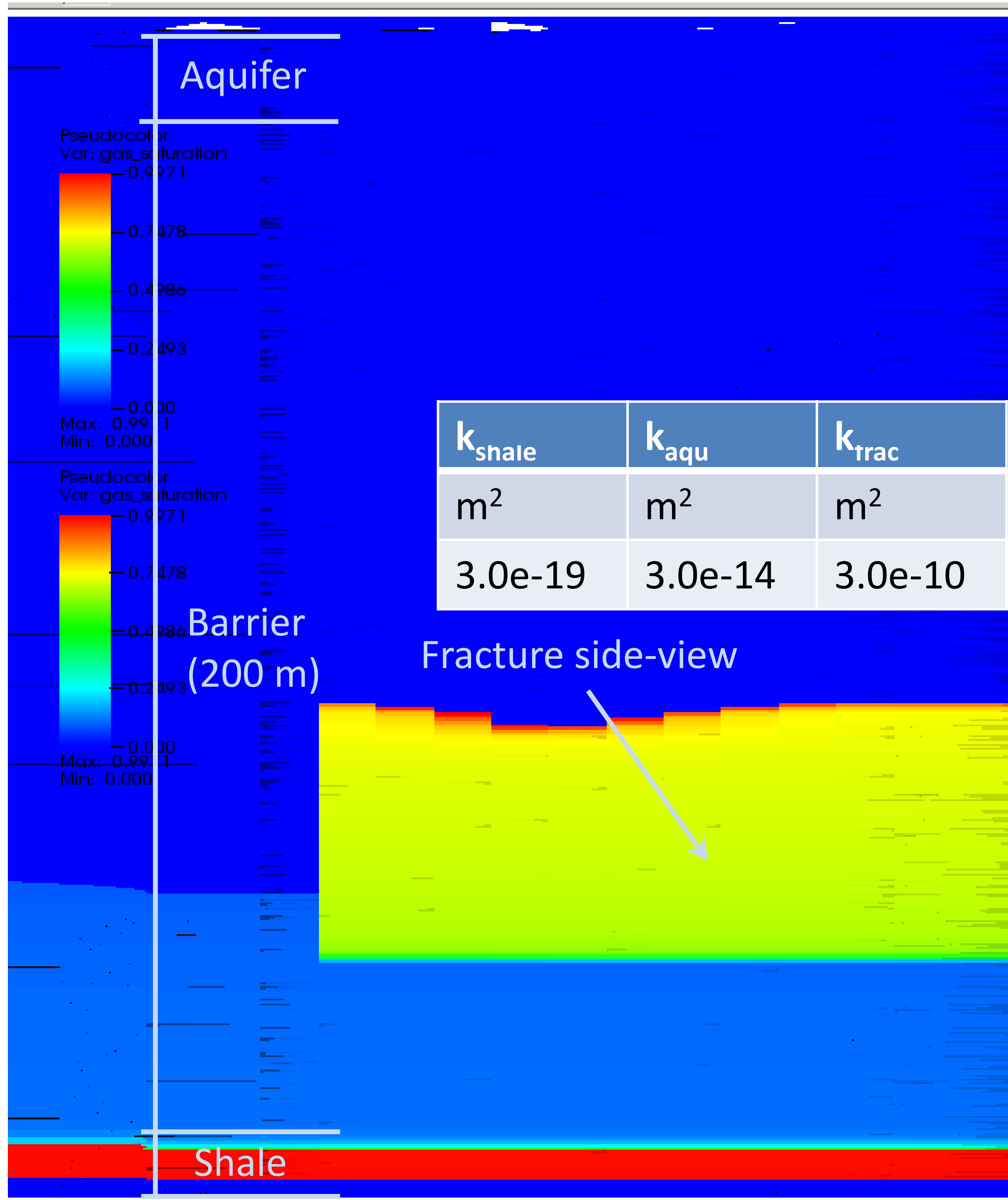

k_{shale}	k_{aqu}	k_{trac}	q_{water}
m^2	m^2	m^2	kg/s
3.0e-19	3.0e-14	3.0e-10	0.0

3000 seconds
Case 161

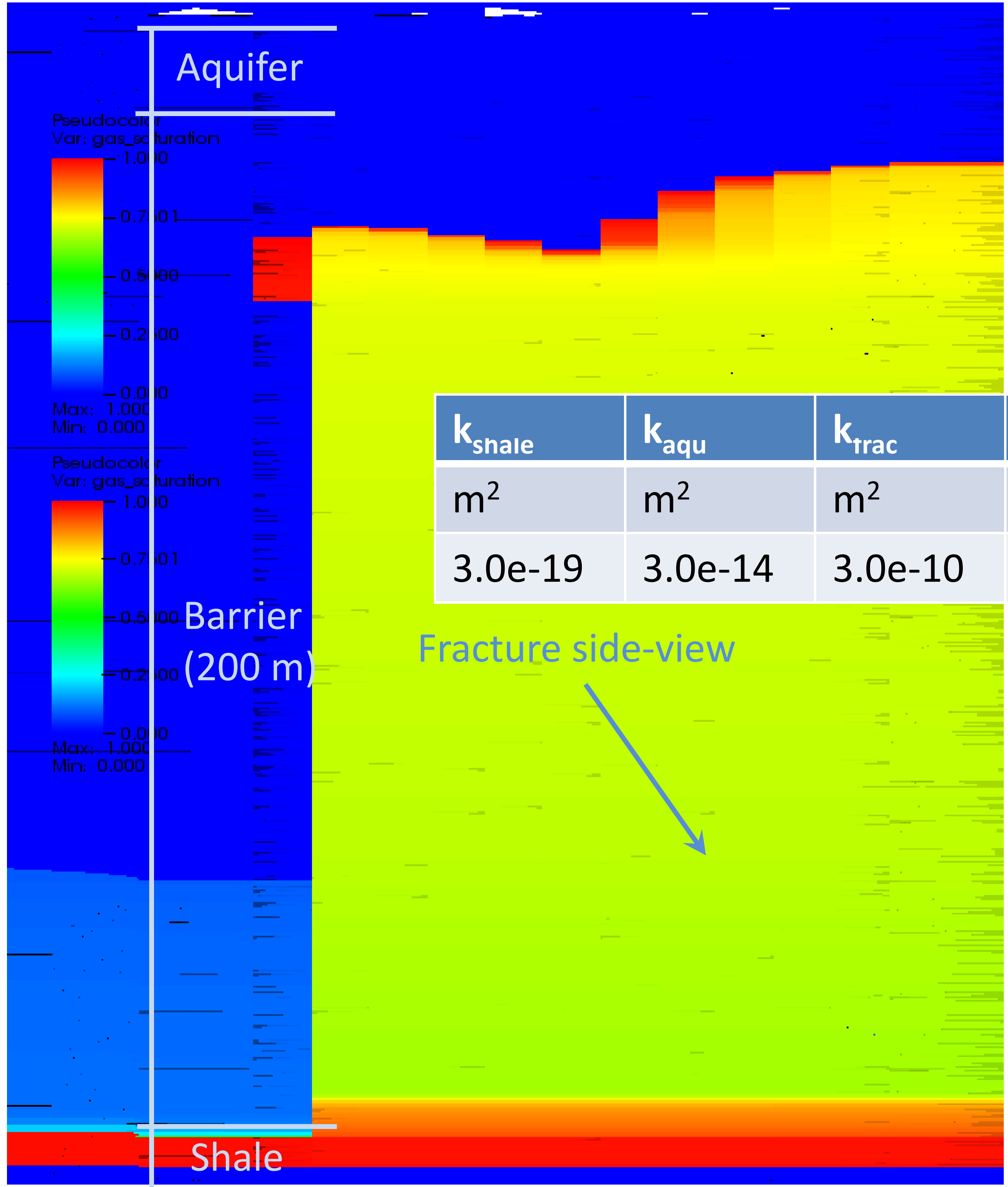

k_{shale}	k_{aqu}	k_{trac}	q_{water}
m^2	m^2	m^2	kg/s
3.0e-19	3.0e-14	3.0e-10	0.0

12000 seconds
Case 161

Conclusions

1) Primary drivers for accelerated gas leakage:
   - Conductivity of the leaking pathway
   - Relative pressure regimes
   - Shale permeability
   - Shale-aquifer separation

Modeling Failure Scenarios: Extensive Fracture Development and Fault Activation

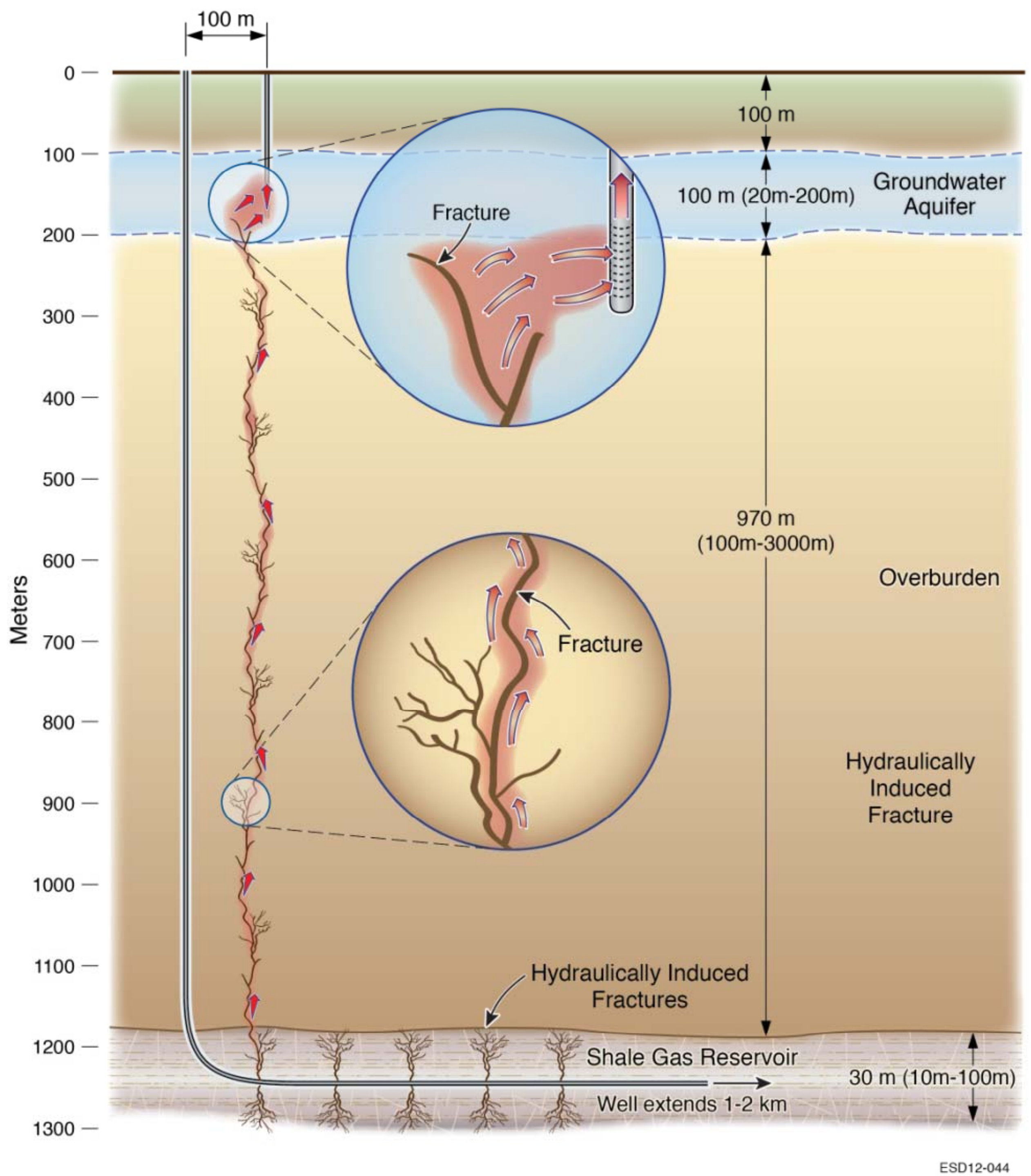

HF extending from shale to shallow aquifer through the overburden

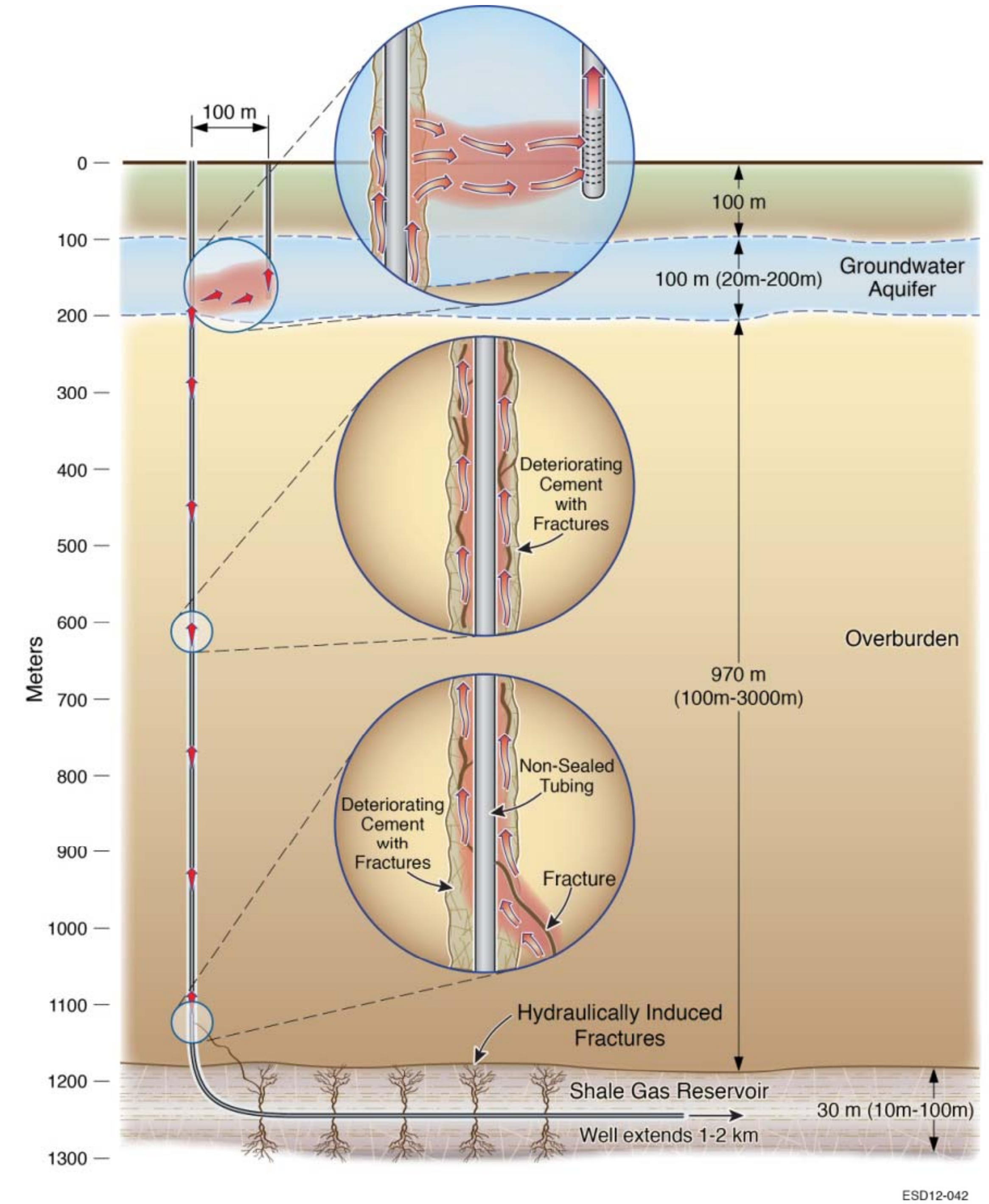

HF extending from shale to shallow aquifer through weak cement (not discussed)

3D Domain

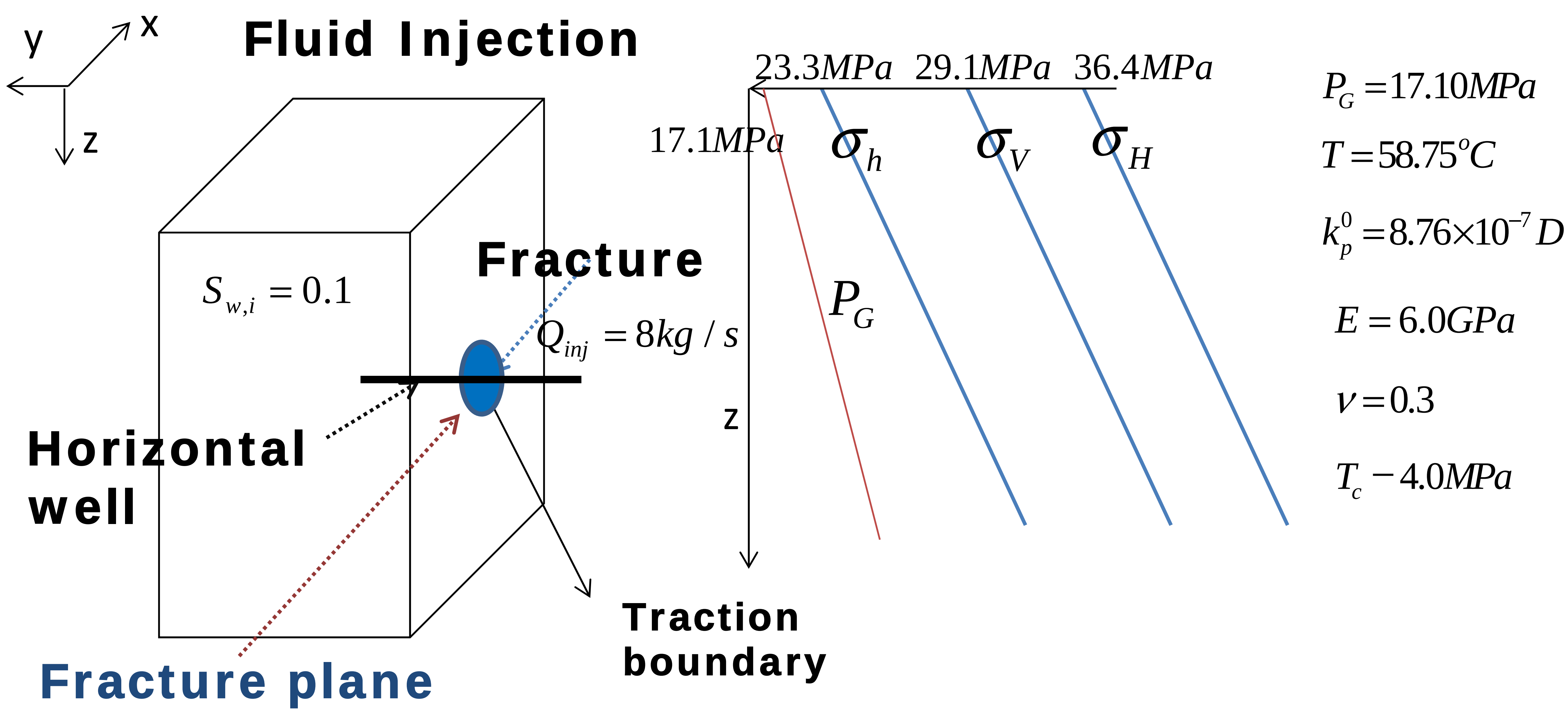

Investigate fracture propagation in shale gas reservoirs - **properties of Marcellus shale**

Fracture Propagation (I)

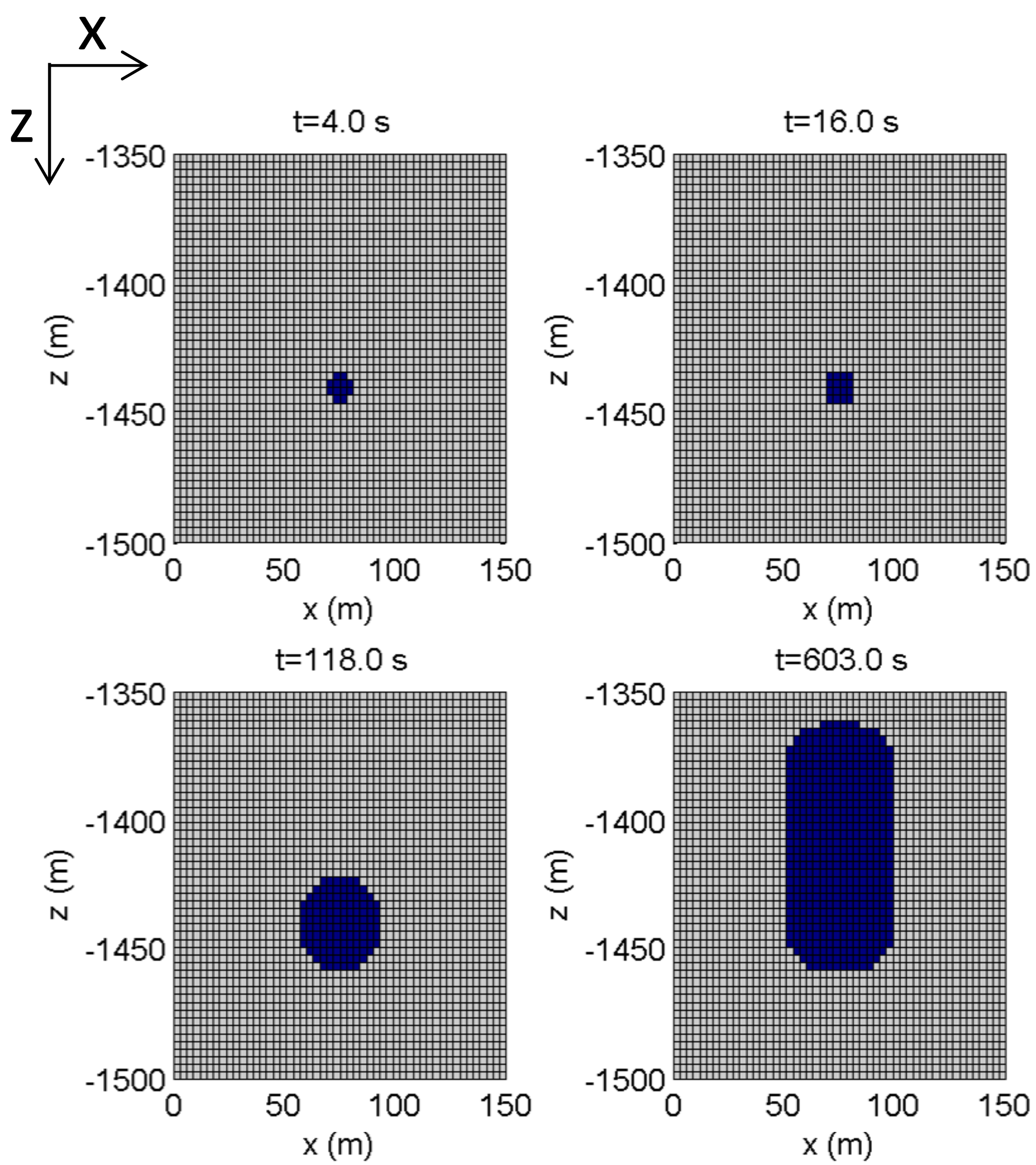

Fractured areas

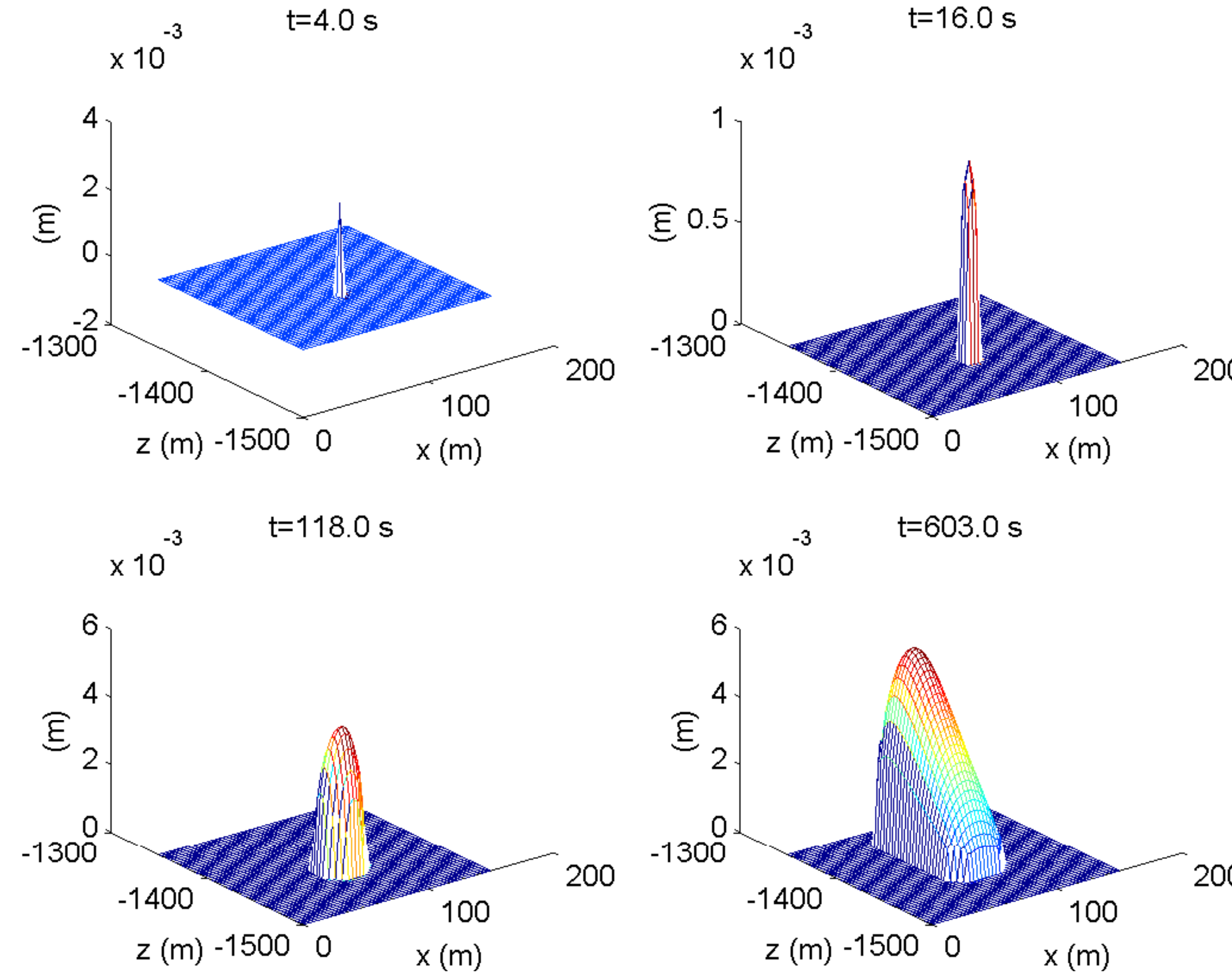

Fracture aperture

Example of fracture propagation

Larger fracture aperture near the fracture top

Effective Stress

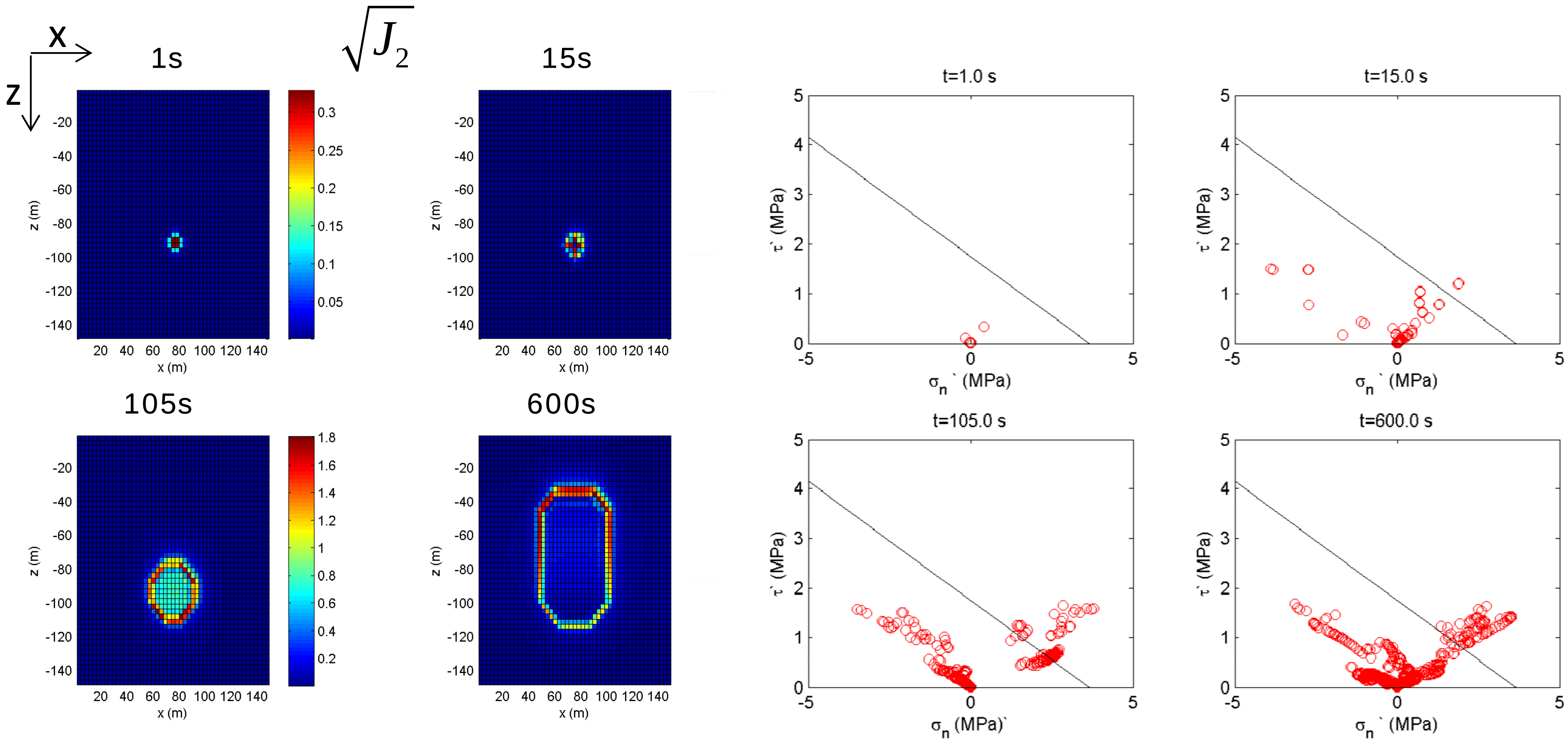

High shear stress near the fracture tips

Shear failure is possible when shear strength is low.

Evolution of Pressure

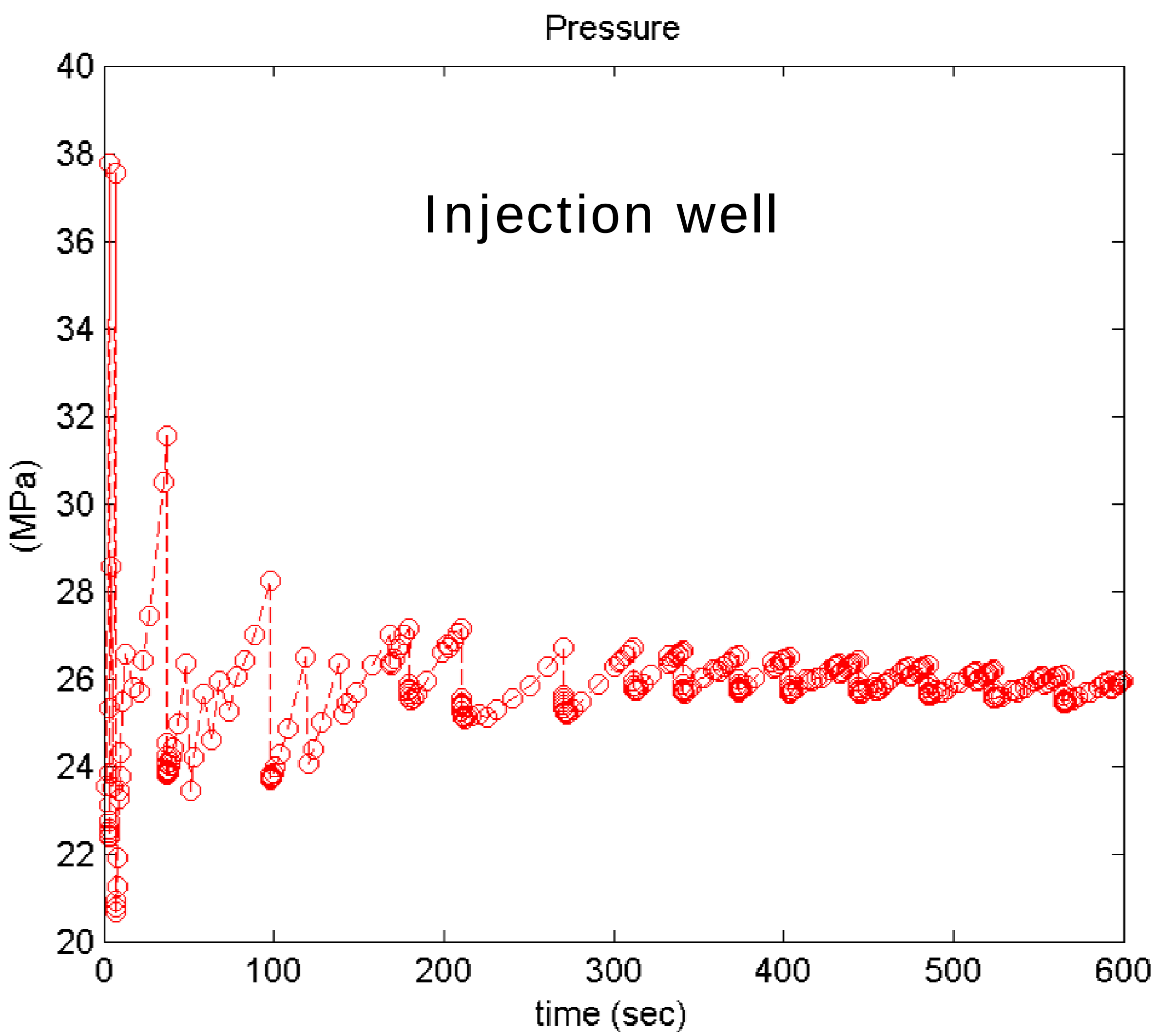

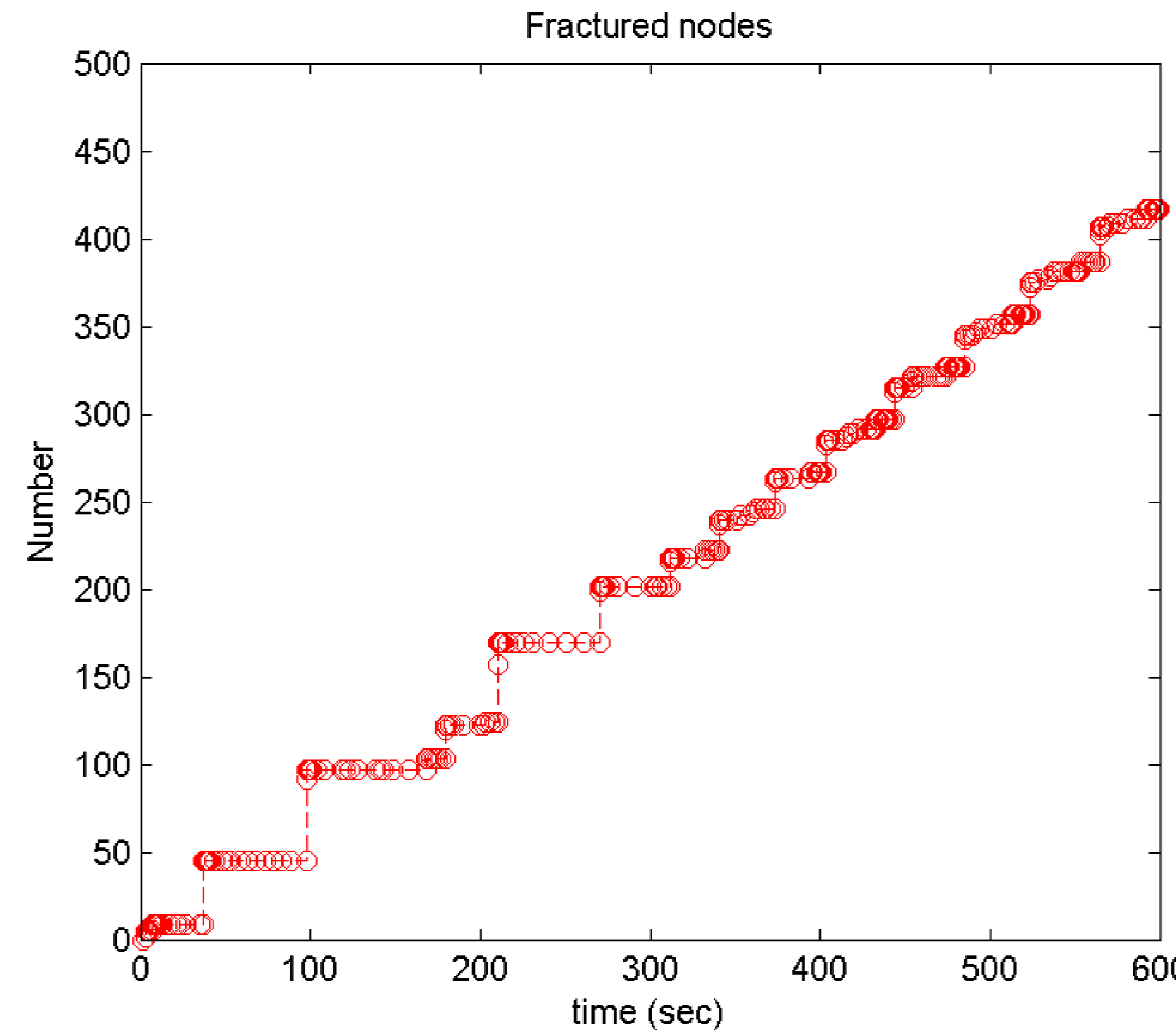

High pressure is required for fracturing, but the pressure decreases at late time

Stable fracture propagation

Fracture Propagation (II)

Fast pressure diffusion due to high permeability

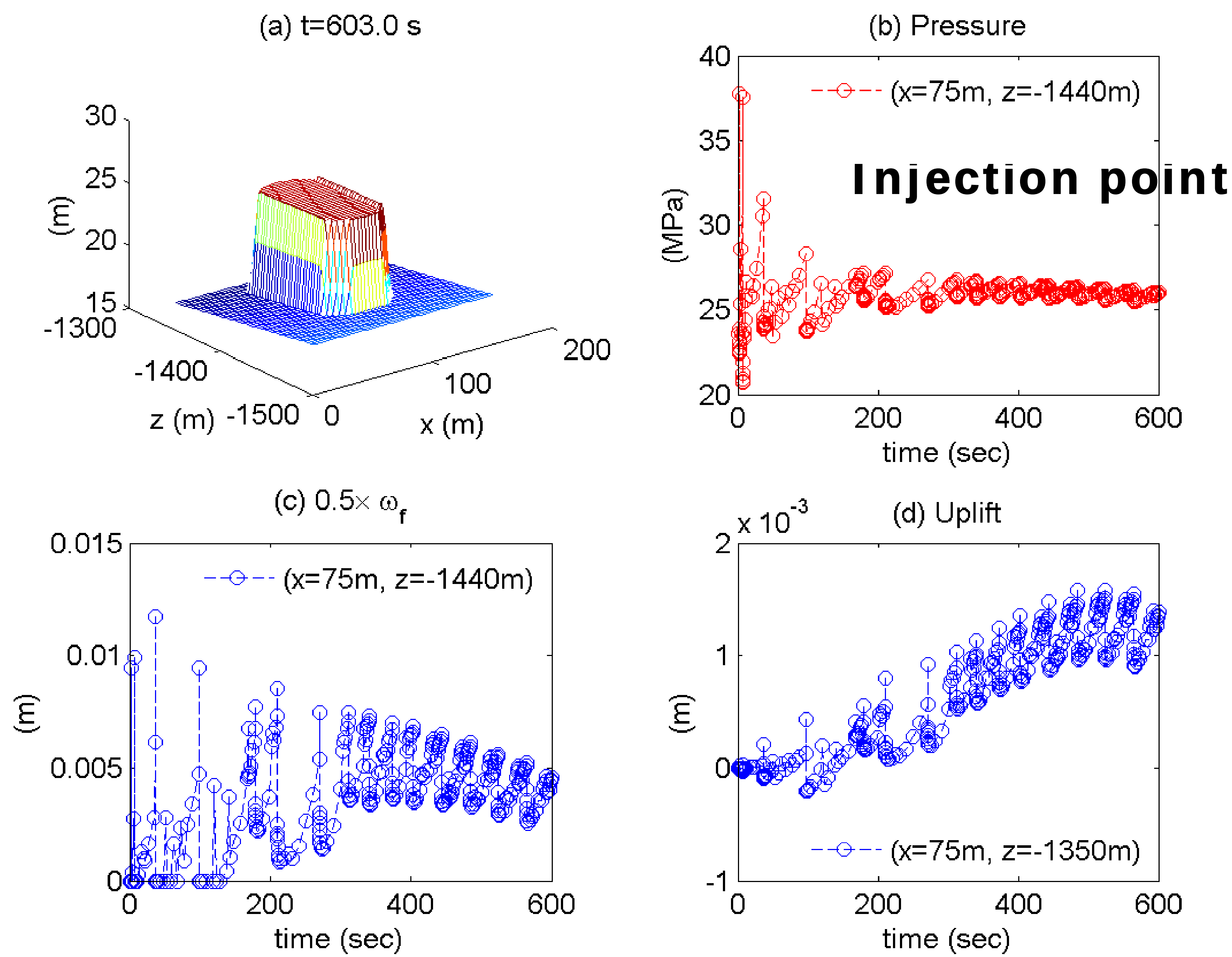

Saw-tooth (oscillatory) pressure, fracture aperture, displacement

Can be considered as **microearthquakes induced by tensile failure**

Shear stress study: an example

High shear stress near the fracture tips

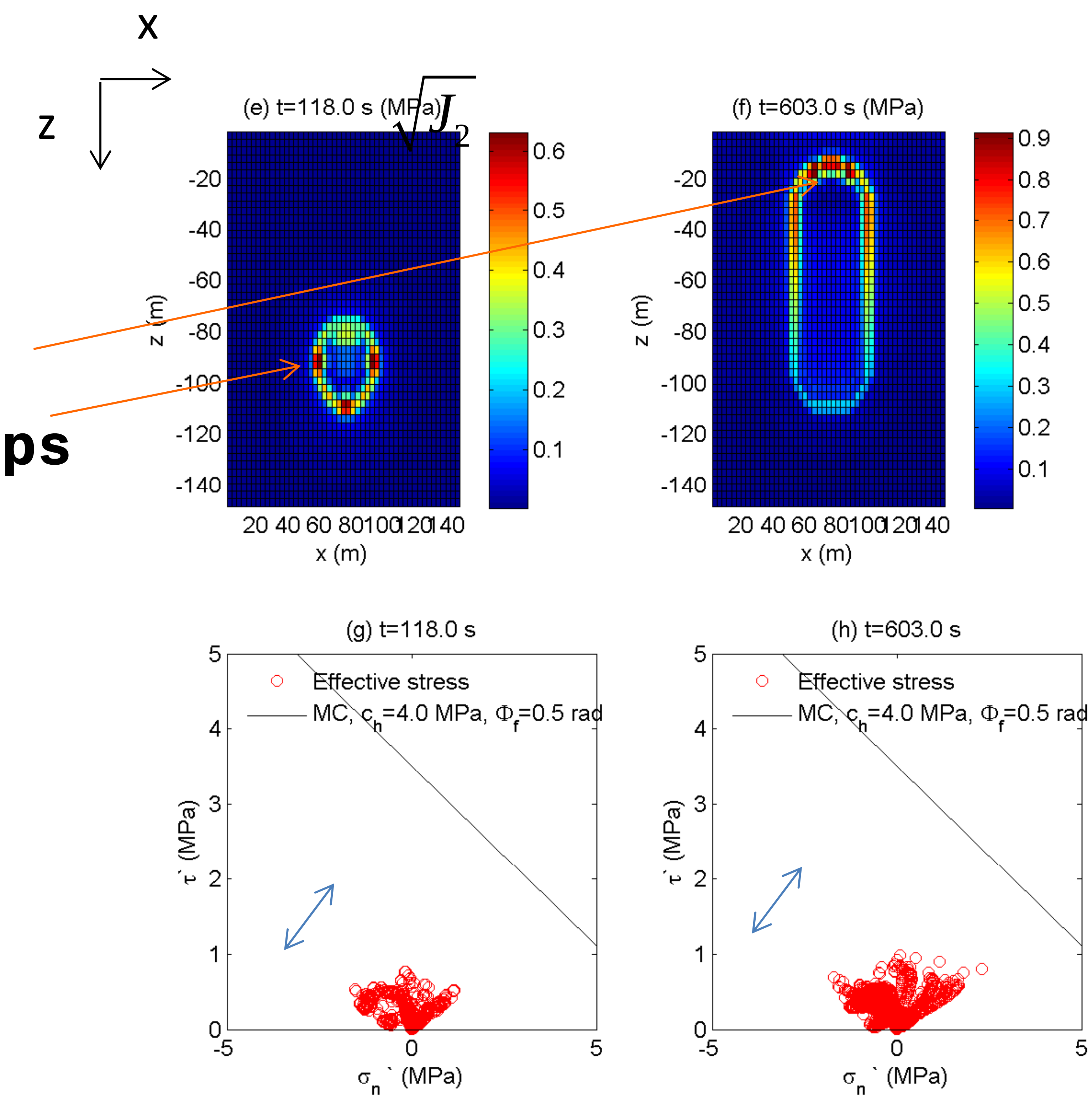

Investigating the probability of shear failure

Coexistence of water & gas

$S_{w,i} = 0.6$

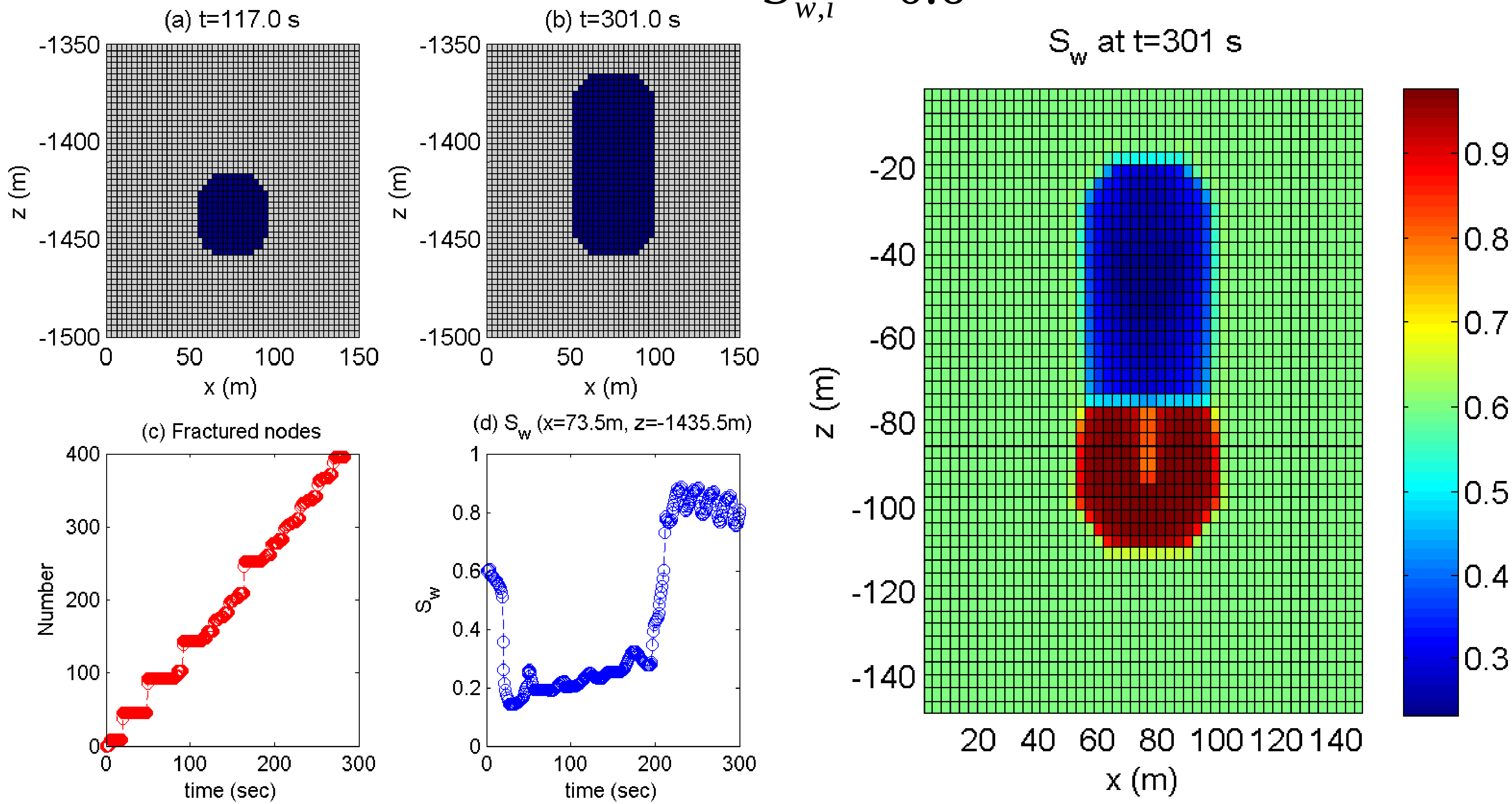

Simple calculation by only the injection volume might significantly underestimate the fracture volume and propagation.

Complex multiphase flow with gravity segregation within the fracture

Water injection: fundamental issues

$S_{w,i} = 0.9$

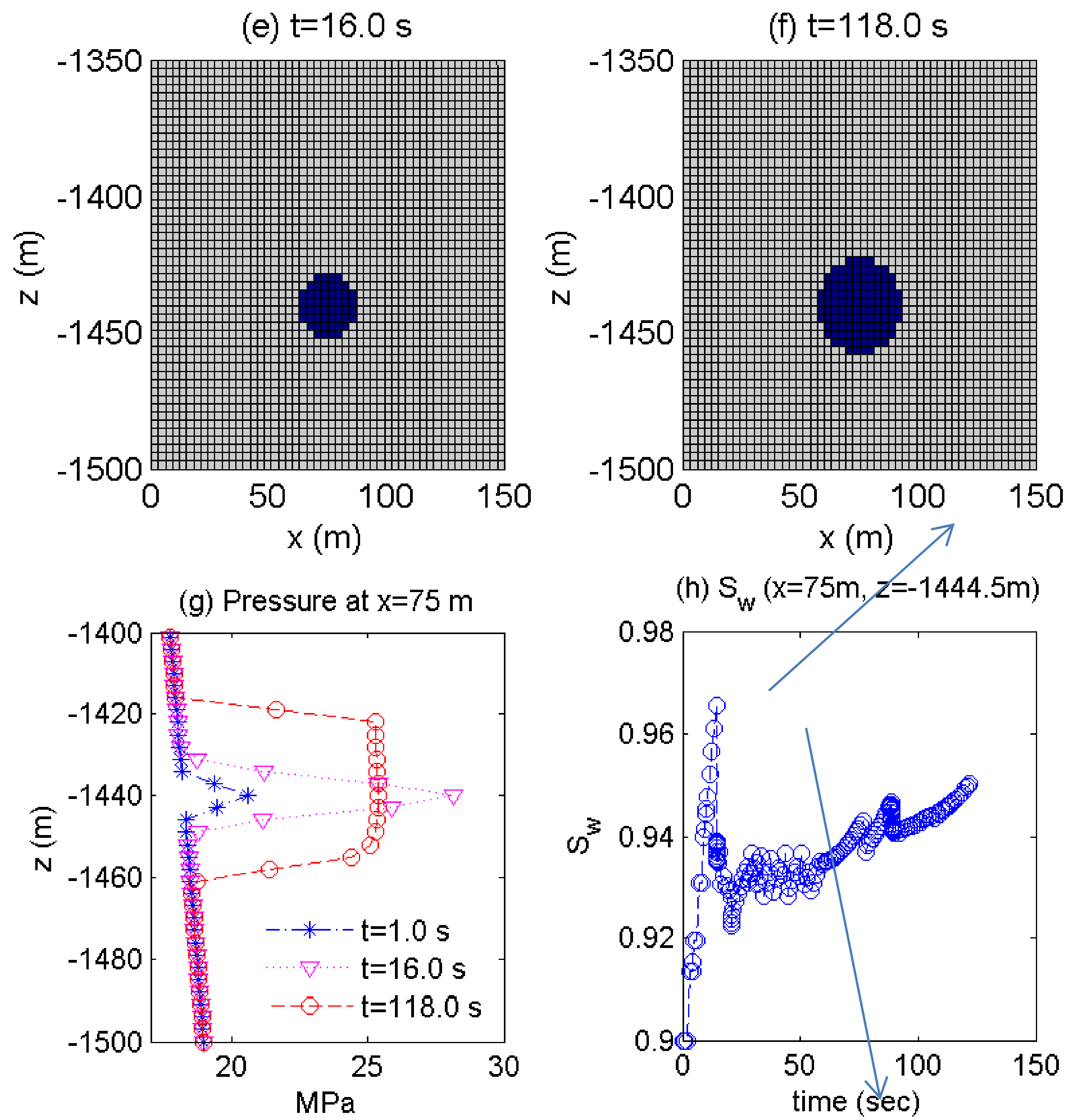

Does not approach
Sw = 1.0

Water & gas still coexist within the fracture.
Water saturation drops at the time when fracturing occurs.

Higher Injection Rate

$$Q_{inj} = 16kg/s$$

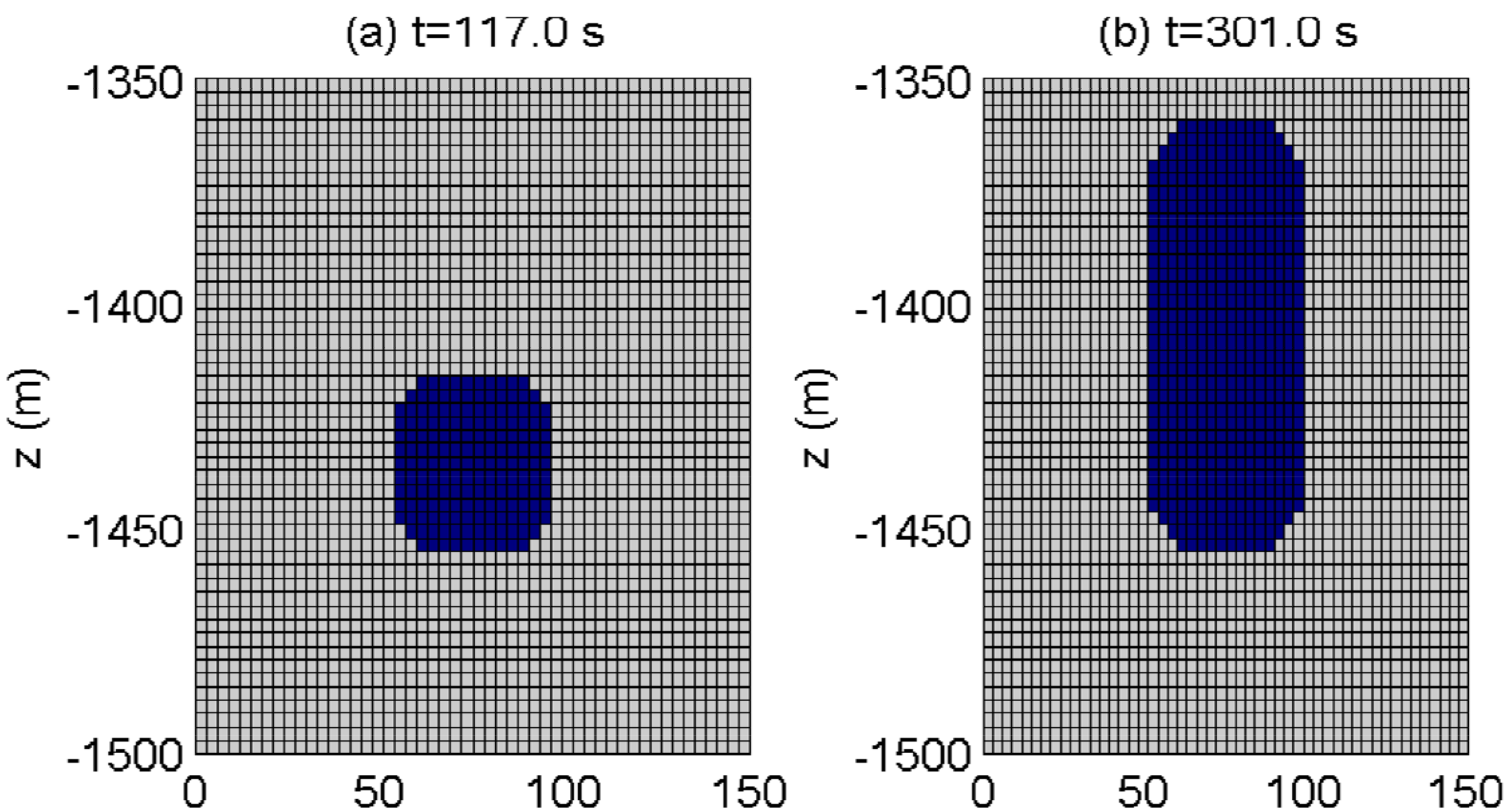

Higher peak pressure

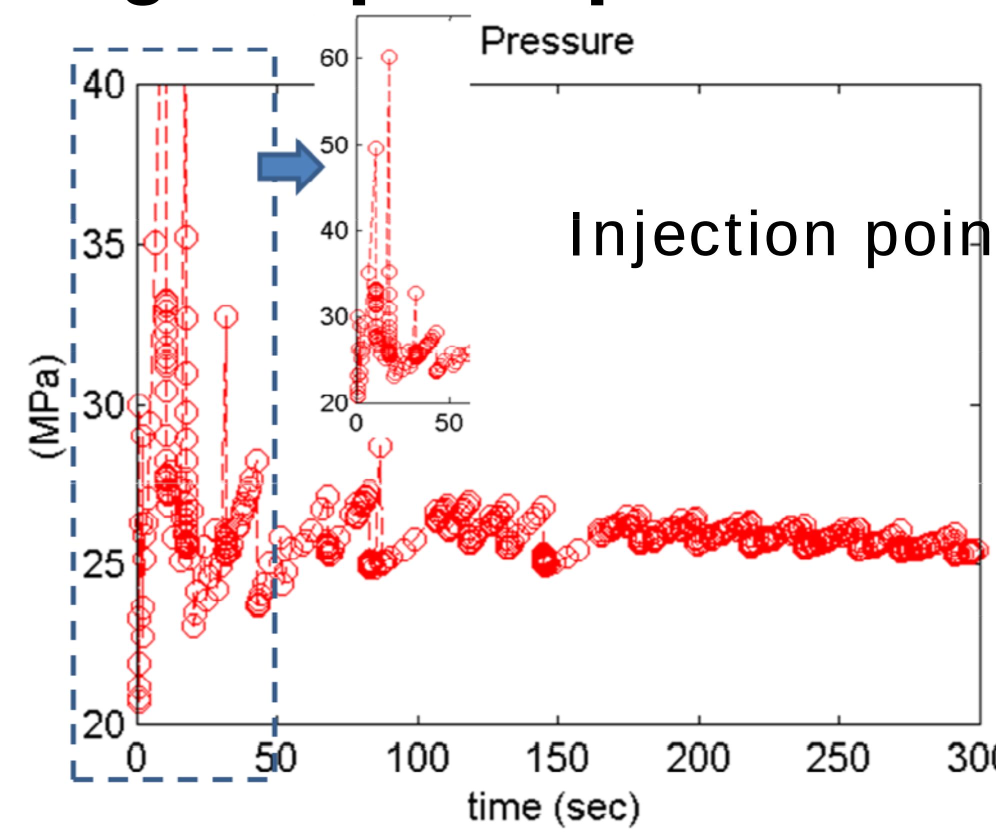

Higher injection rate = faster fracture propagation

Maximum Horizontal Stress, S_H

$$S_H = 1.2 \times S_V$$

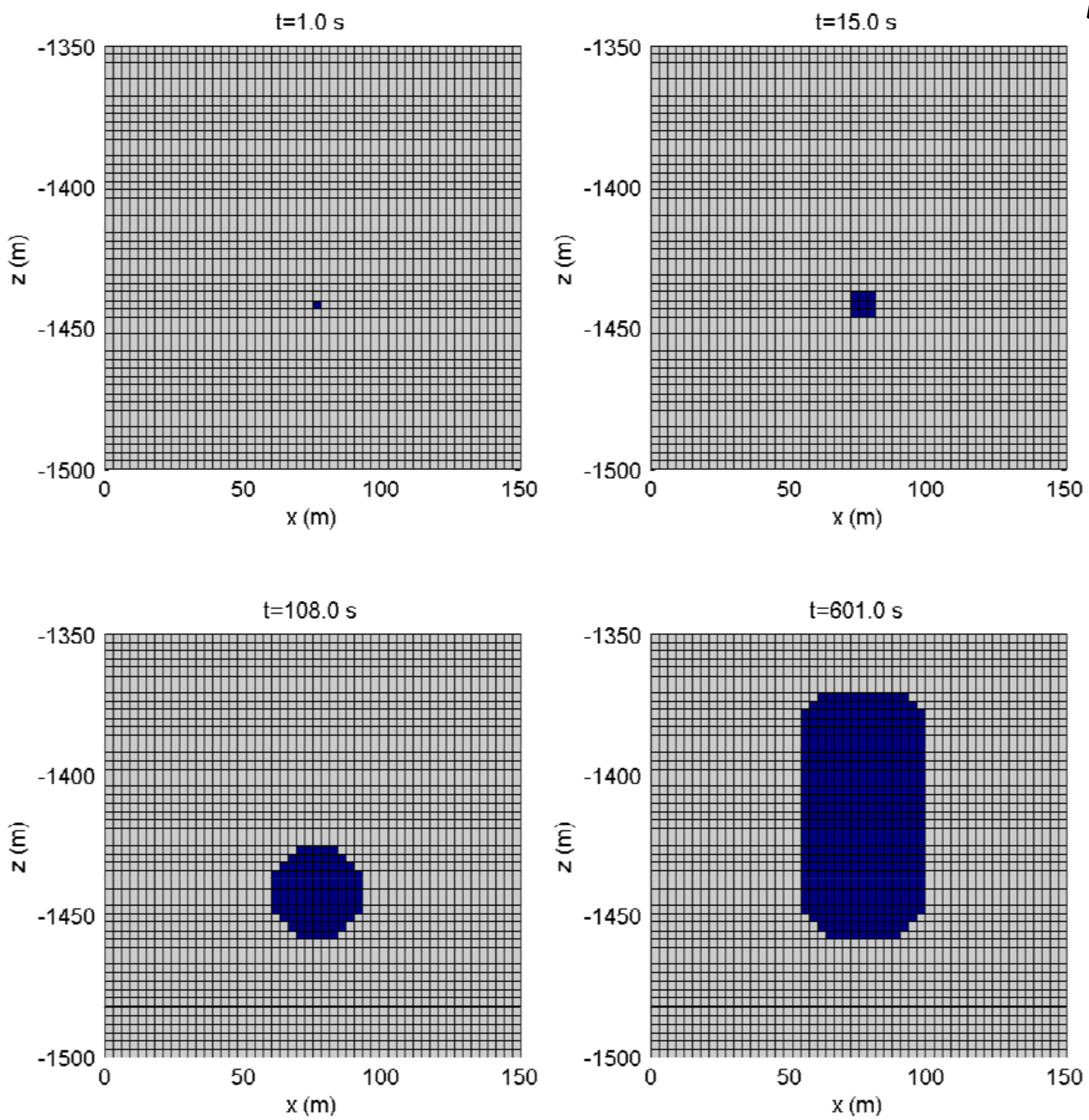

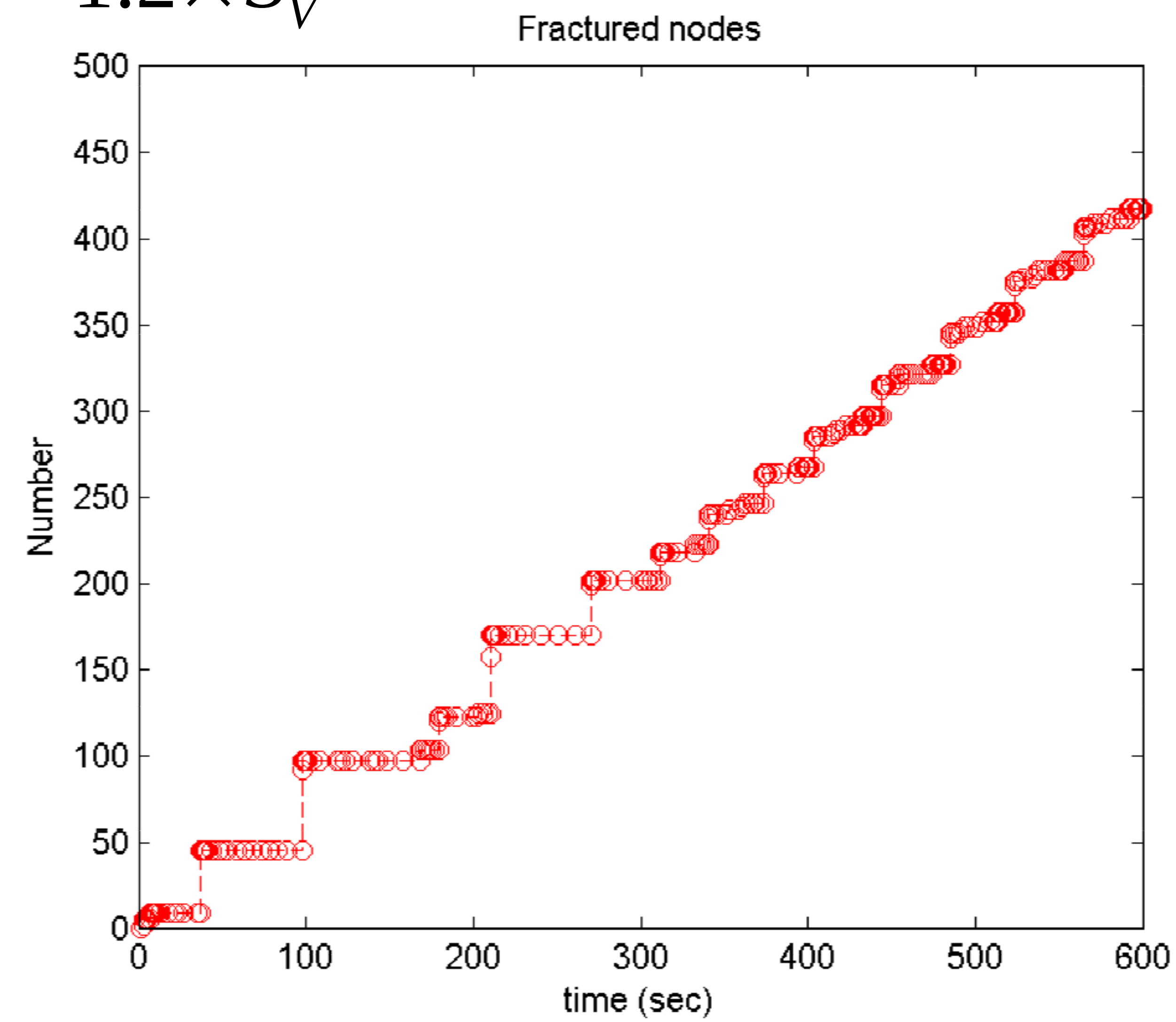

Change in S_H induces slight change in the fracture shape.

Heterogeneity effects

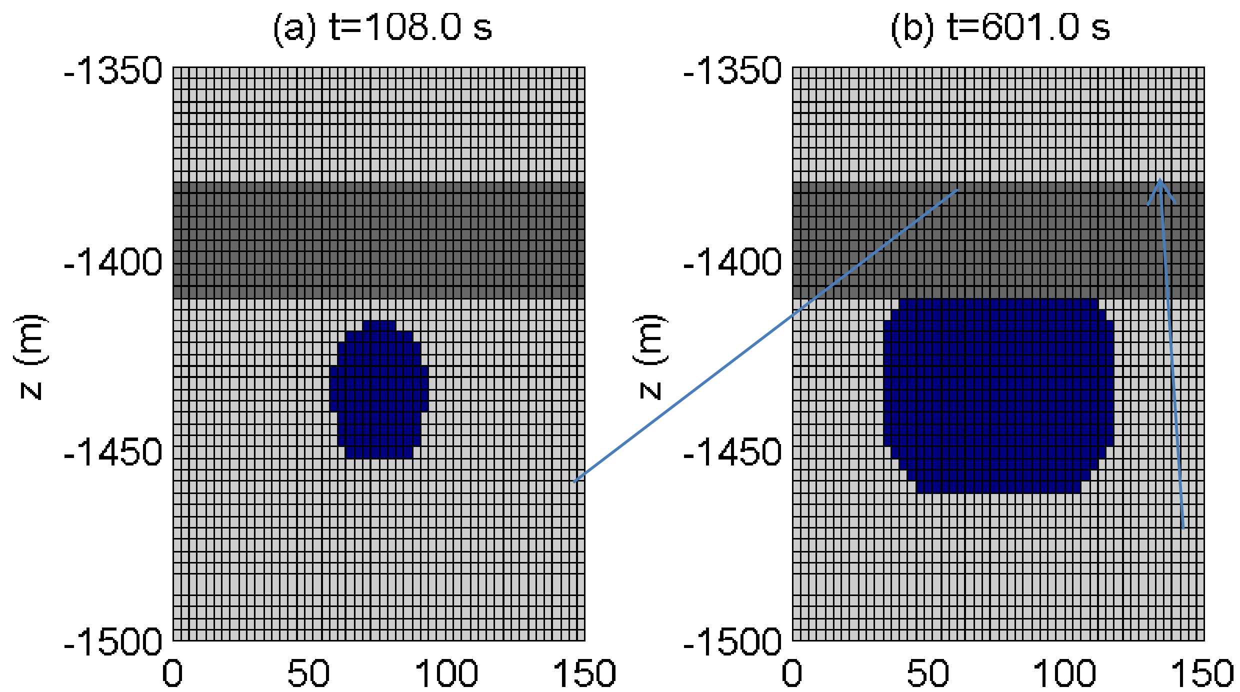

A strong geological formation with τ_c = 10 MPa

A strong geological formation can block vertical fracture propagation

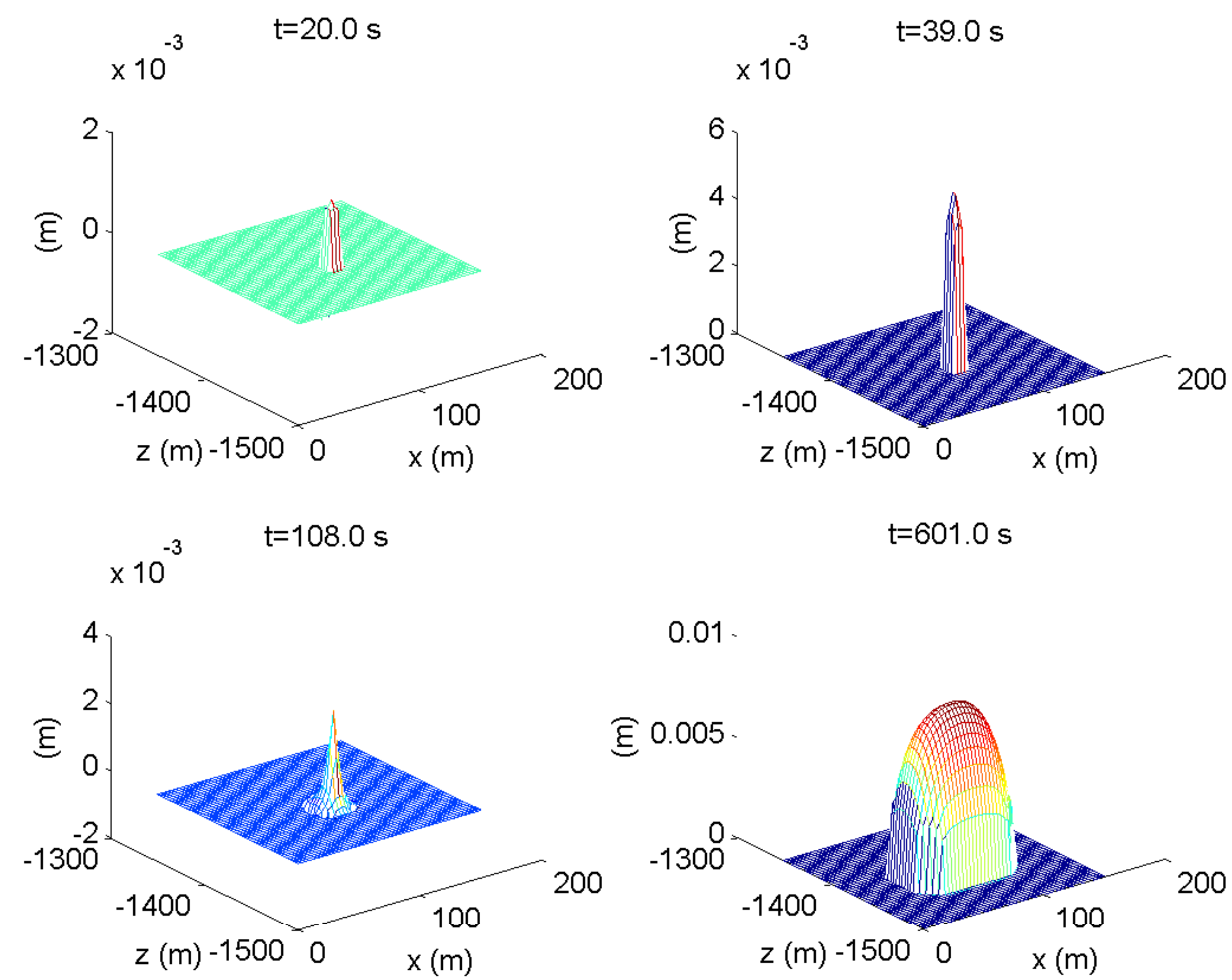

Failure scenarios (?)

Fault activation during the hydraulic fracturing process

Code:
TOUGH+ RealGasH2O+ FLAC3d

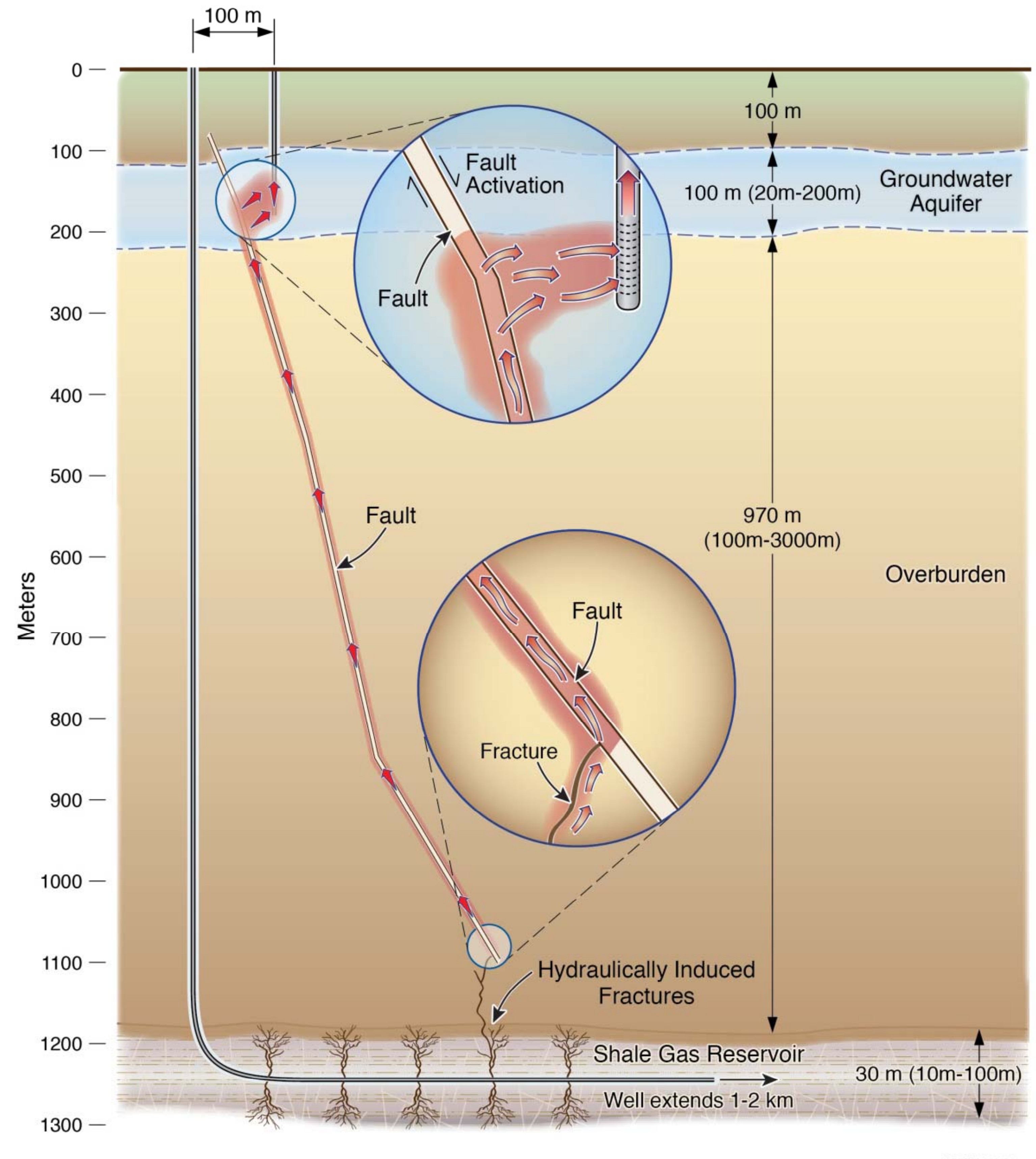

Constant rate of P-increase

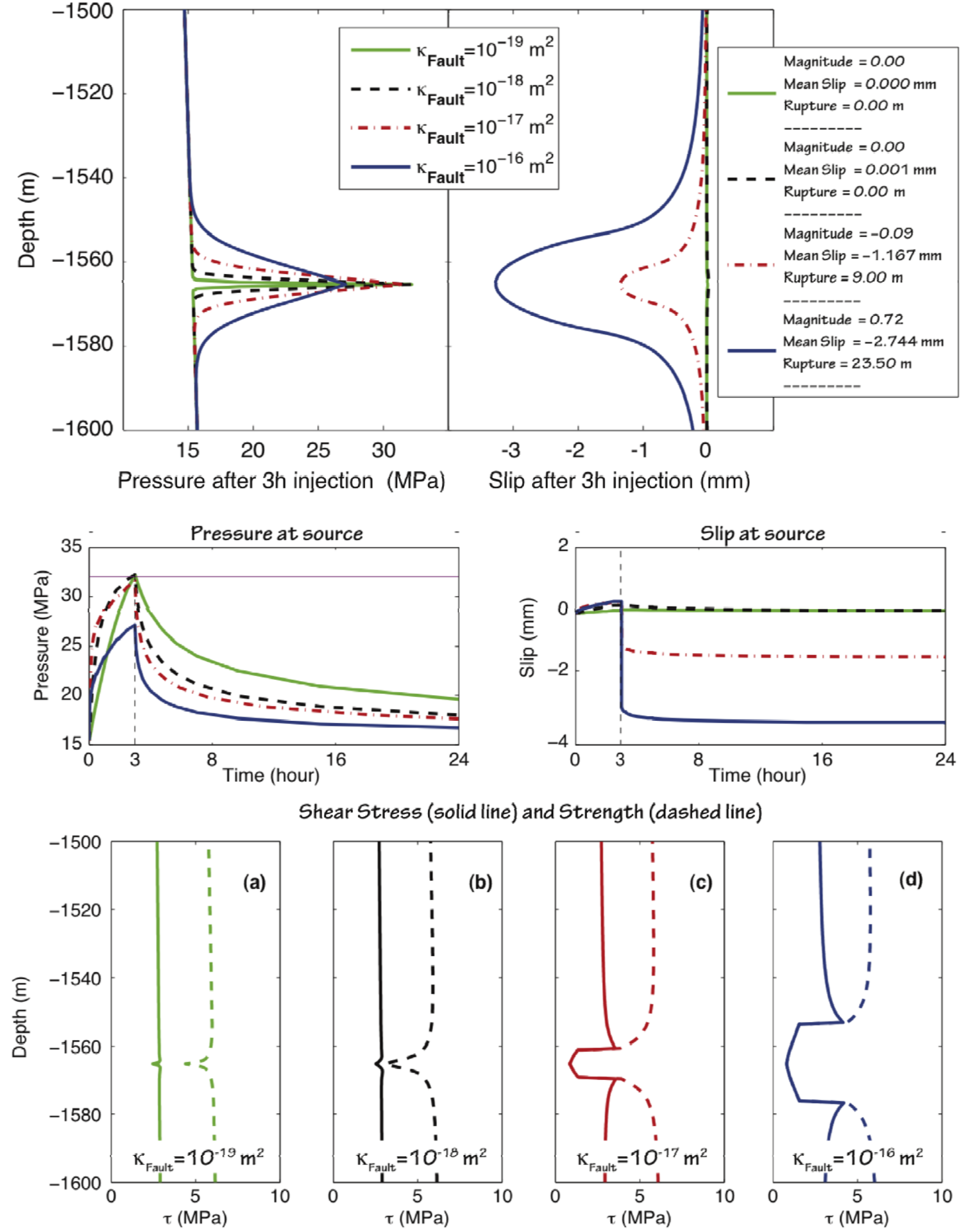

Constant rate of injection

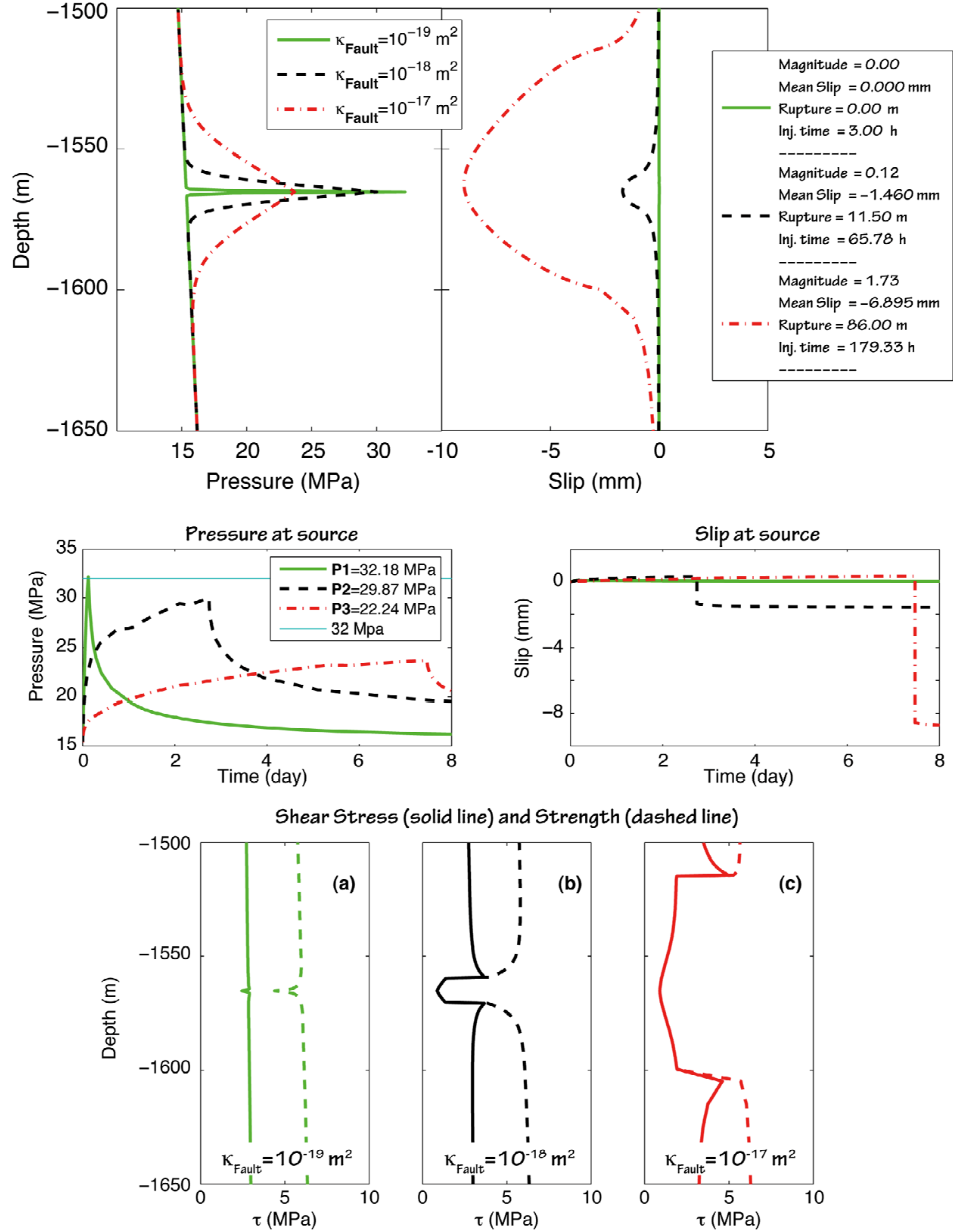

Conclusions

- Developed a hydraulic fracturing simulator
- Investigated fracture propagation scenarios in Marcellus shales
- Identifying the factors controlling fracture propagation
- Estimation based on the injection volume may significantly underestimate the fracture volume & its propagation

⇨ Rigorous modeling of fracture propagation & accurate geophysical monitoring are strongly recommended

Acknowledgements

- The research described in this article has been funded by the U.S. Environmental Protection Agency through Interagency Agreement (DW-89-92235901-C) to the Lawrence Berkeley National Laboratory, and by the Research Partnership to Secure Energy for America (RPSEA - Contract No. 08122-45) through the Ultra-Deepwater and Unconventional Natural Gas and Other Petroleum Resources Research and Development Program as authorized by the US Energy Policy Act (EPAct) of 2005. The views expressed in this article are those of the author(s) and do not necessarily reflect the views or policies of the EPA.

Thank you